Title: Self-force via m-mode regularization and time domain evolution

Date: Jun 20, 2010 09:10 AM

URL: http://pirsa.org/10060033

Abstract: TBA

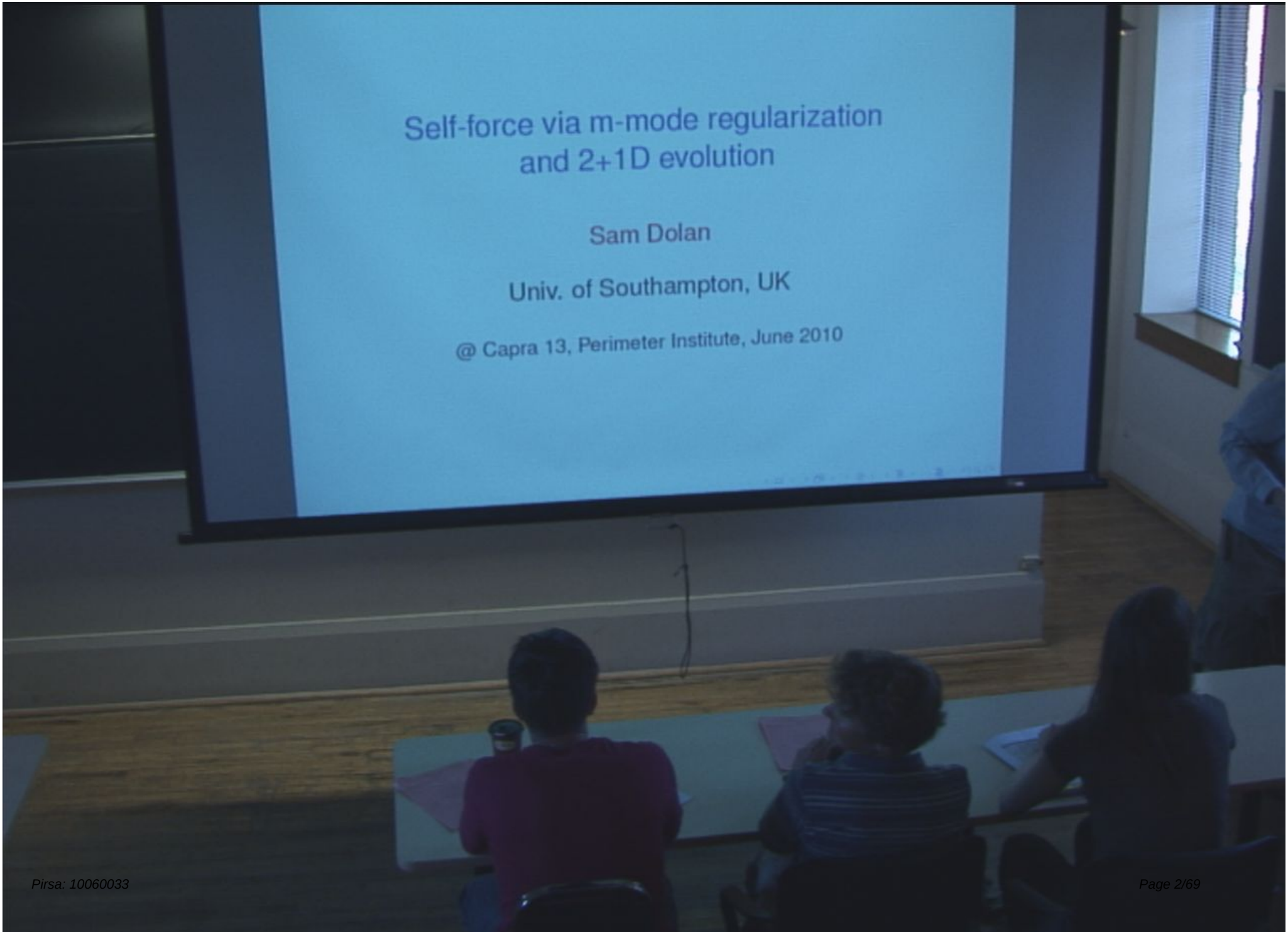
Self-force via m-mode regularization
and 2+1D evolution
Sam Dolan
Univ. of Southampton, UK
@ Capra 13, Perimeter Institute, June 2010

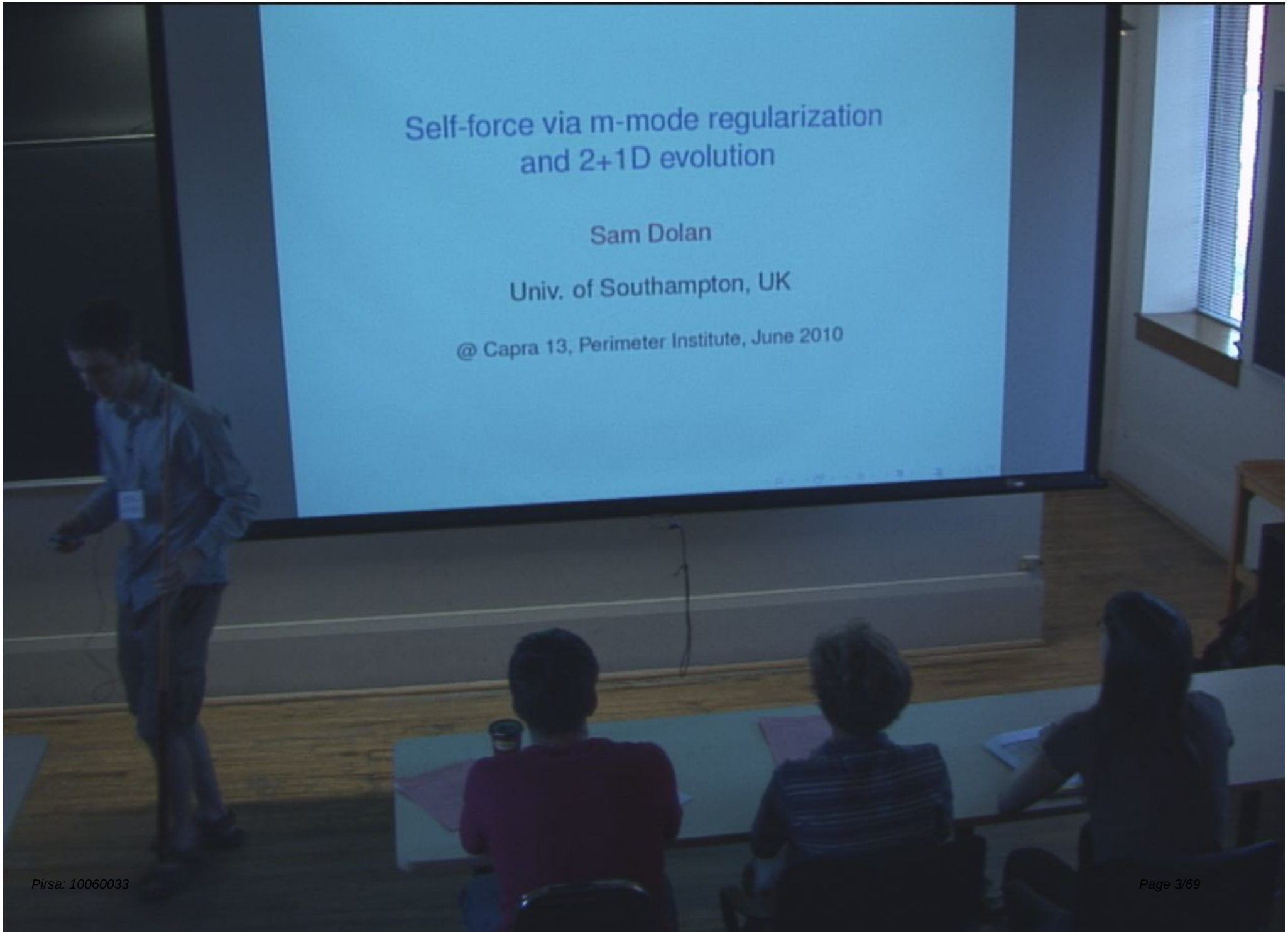
Self-force via m-mode regularization
and 2+1D evolution
Sam Dolan
Univ. of Southampton, UK
@ Capra 13, Perimeter Institute, June 2010

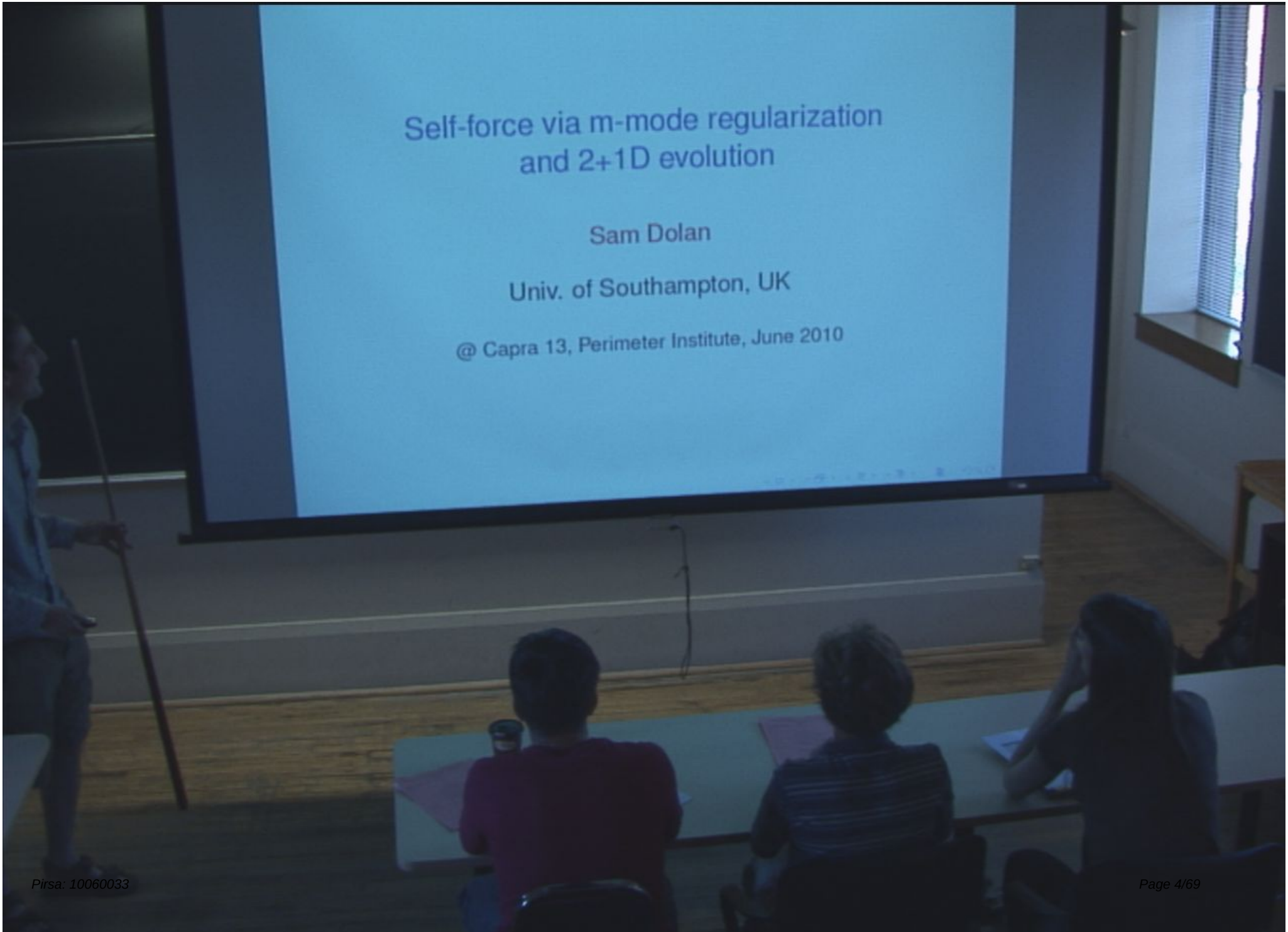
Self-force via m-mode regularization
and 2+1D evolution
Sam Dolan
Univ. of Southampton, UK
@ Capra 13, Perimeter Institute, June 2010

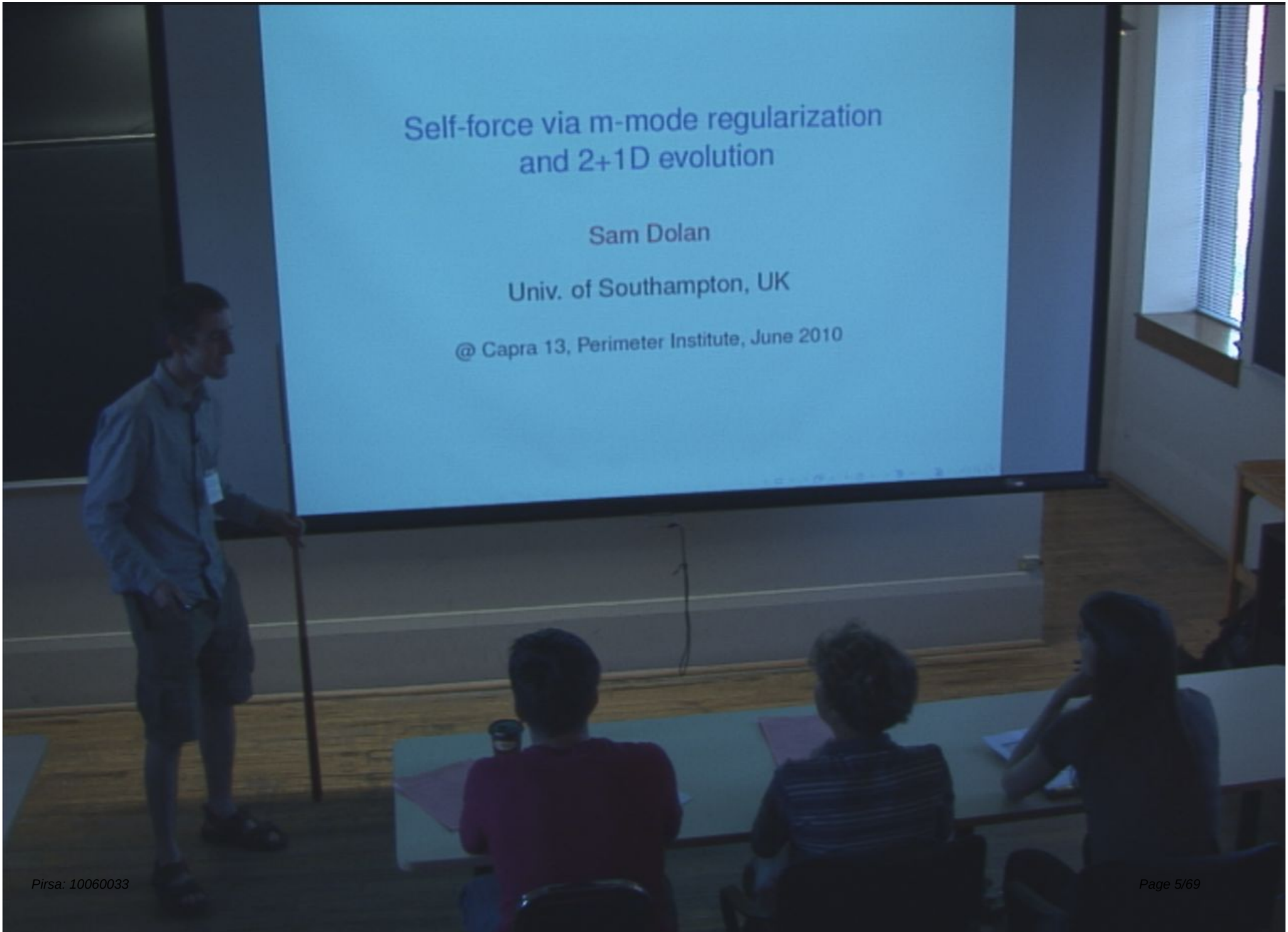
Self-force via m-mode regularization
and 2+1D evolution
Sam Dolan
Univ. of Southampton, UK
@ Capra 13, Perimeter Institute, June 2010

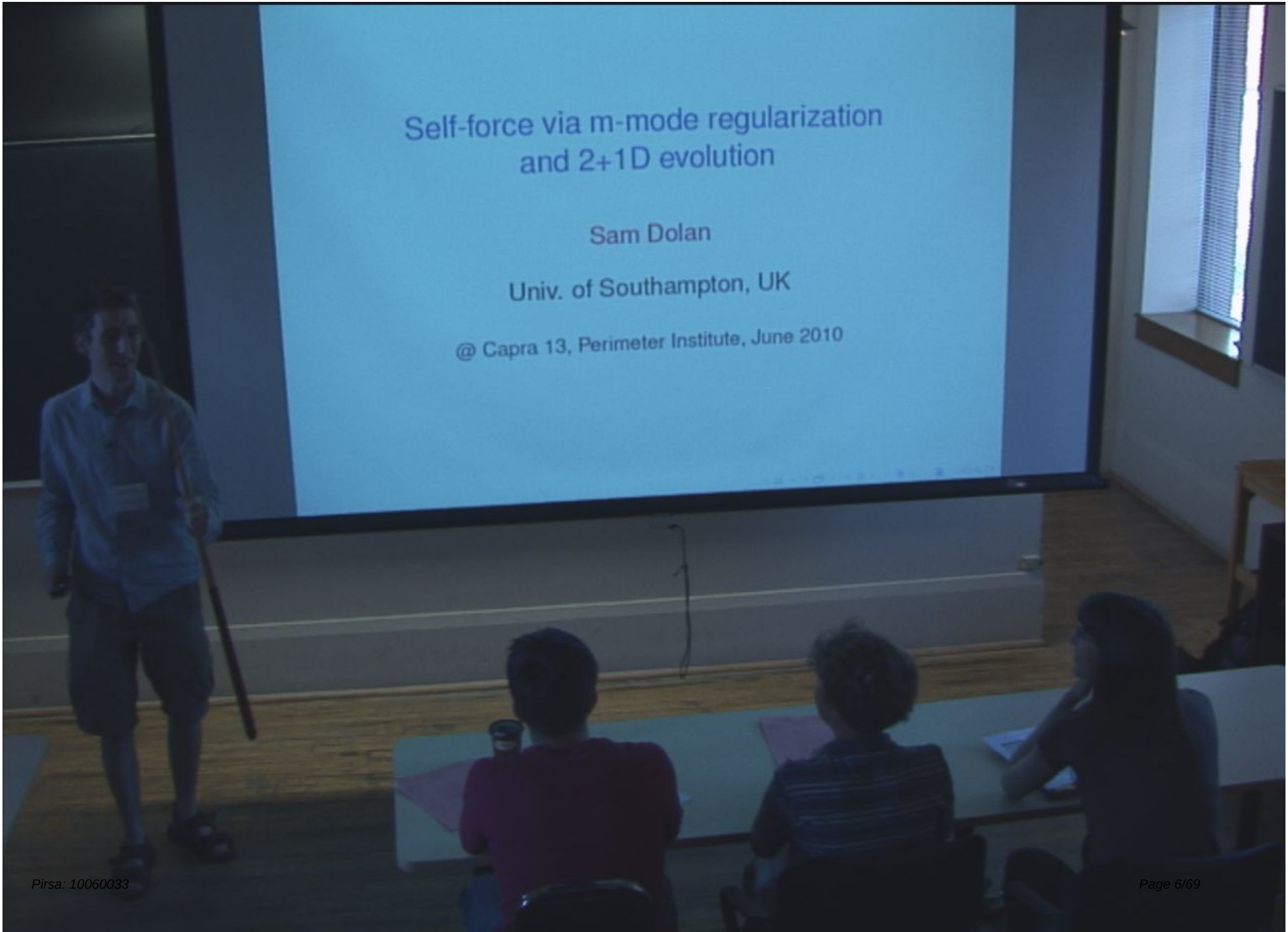
Self-force via m-mode regularization
and 2+1D evolution
Sam Dolan
Univ. of Southampton, UK
@ Capra 13, Perimeter Institute, June 2010

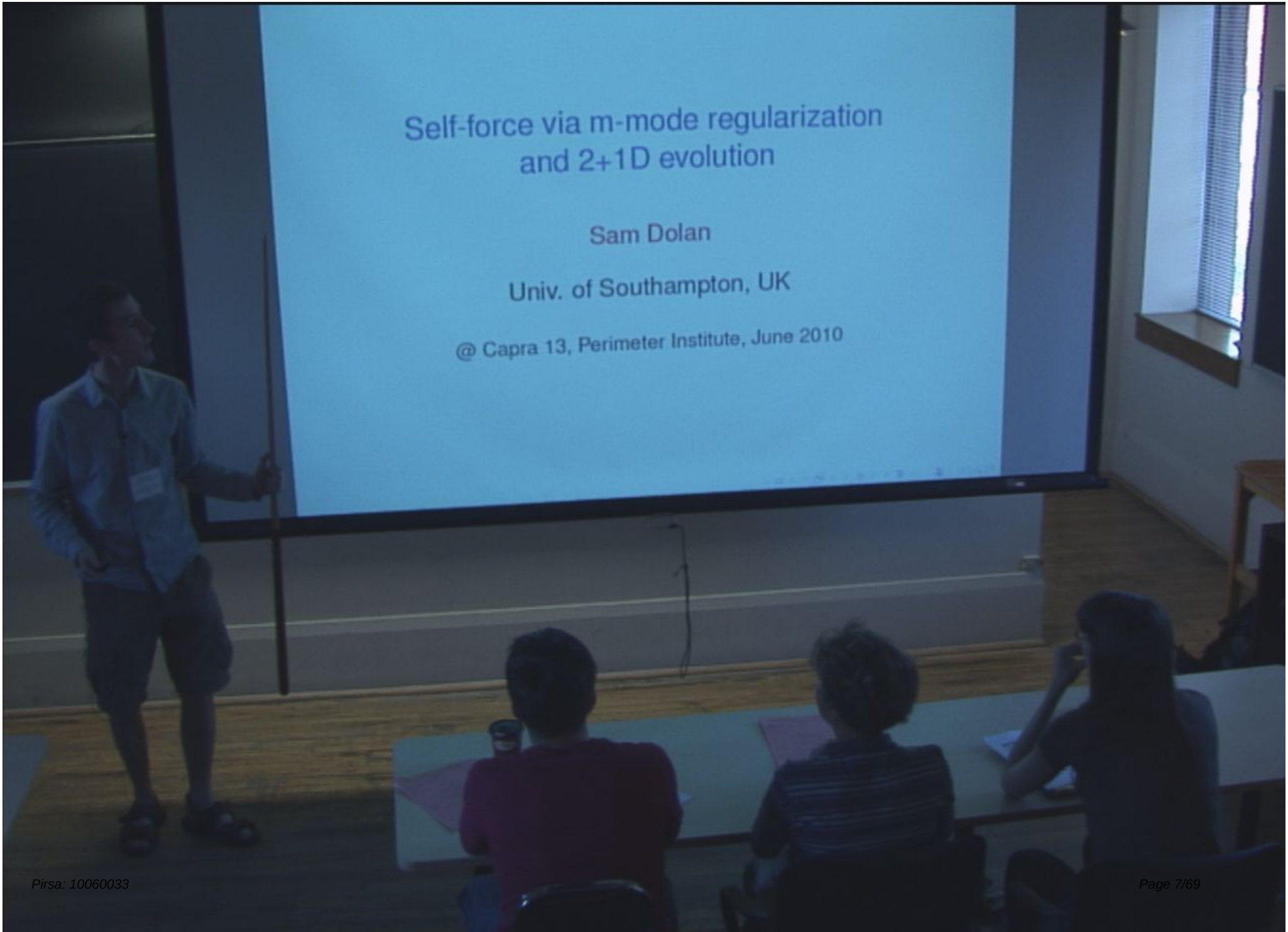
Self-force via m-mode regularization
and 2+1D evolution
Sam Dolan
Univ. of Southampton, UK
@ Capra 13, Perimeter Institute, June 2010

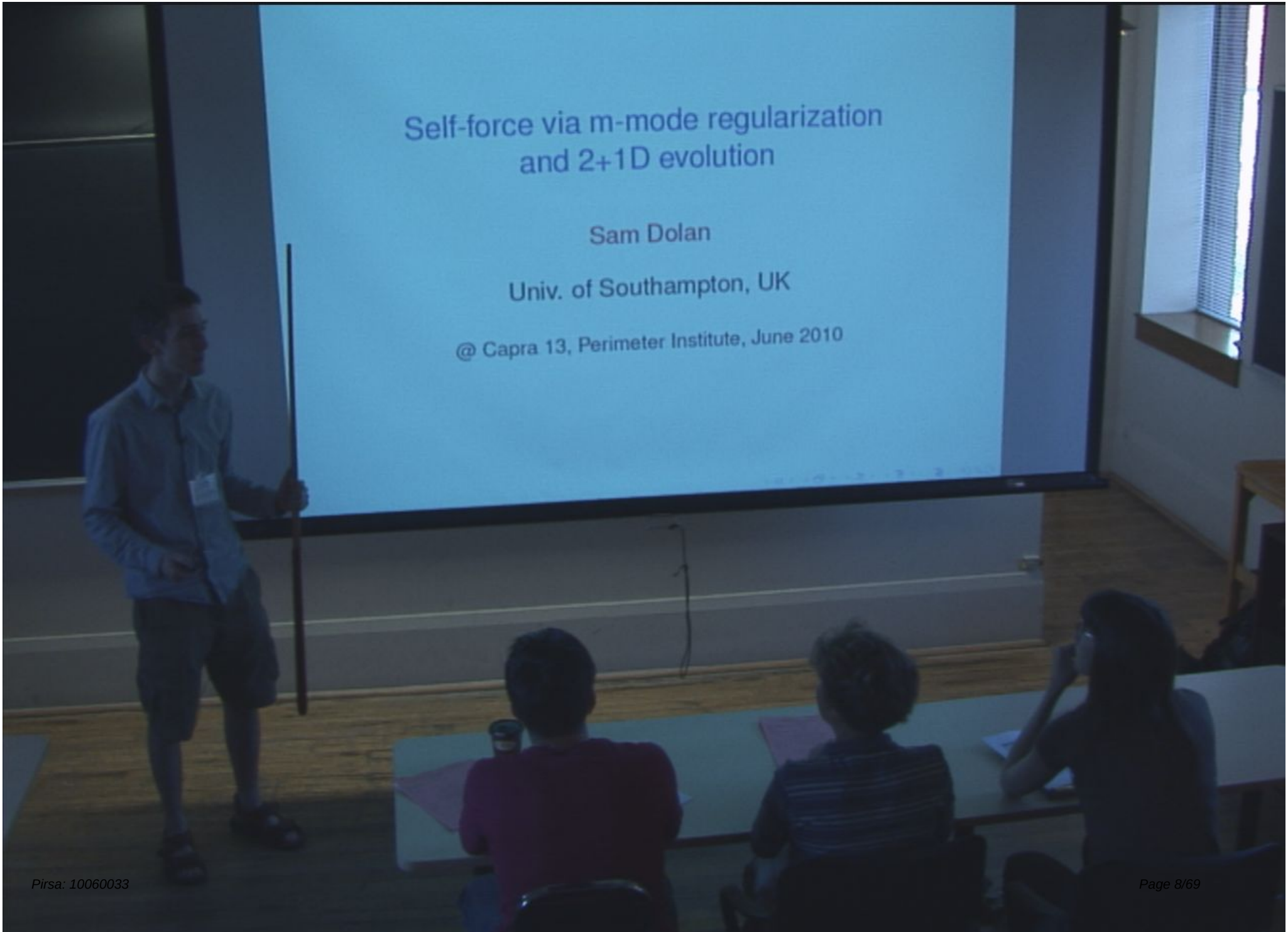
Self-force via m-mode regularization
and 2+1D evolution
Sam Dolan
Univ. of Southampton, UK
@ Capra 13, Perimeter Institute, June 2010

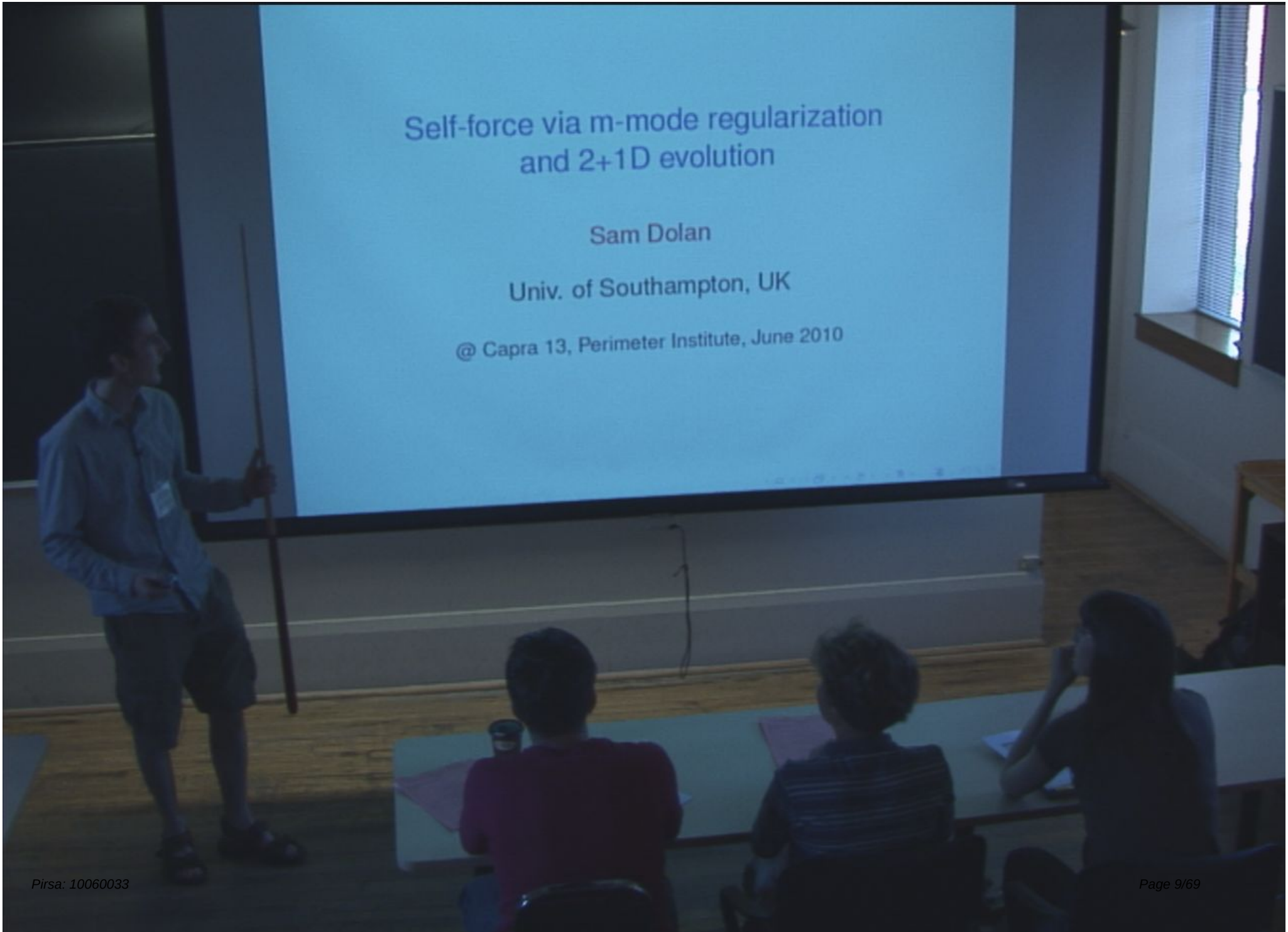
Self-force via m-mode regularization
and 2+1D evolution
Sam Dolan
Univ. of Southampton, UK
@ Capra 13, Perimeter Institute, June 2010

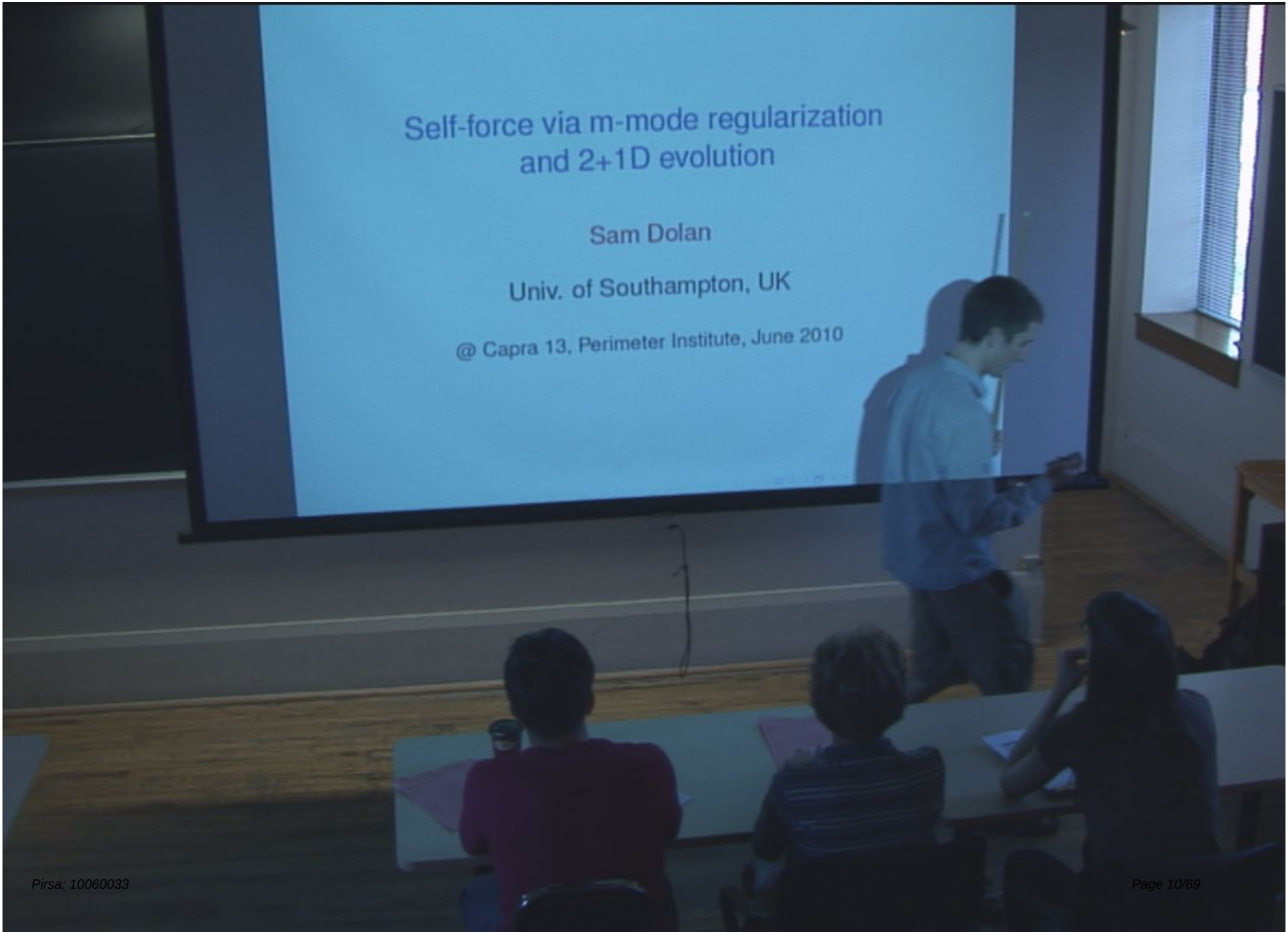
Self-force via m-mode regularization
and 2+1D evolution
Sam Dolan
Univ. of Southampton, UK
@ Capra 13, Perimeter Institute, June 2010

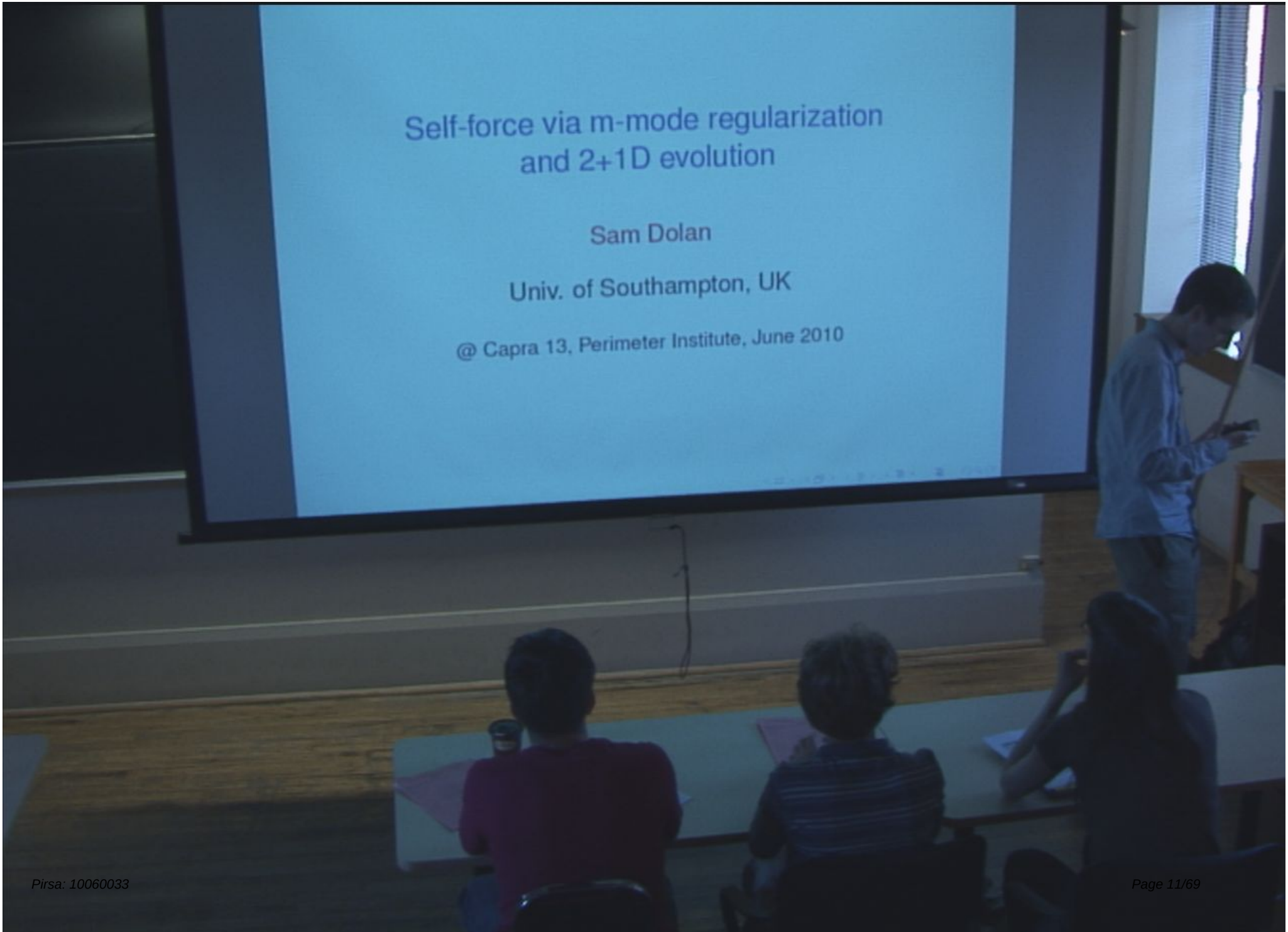
Self-force via m-mode regularization
and 2+1D evolution
Sam Dolan
Univ. of Southampton, UK
@ Capra 13, Perimeter Institute, June 2010

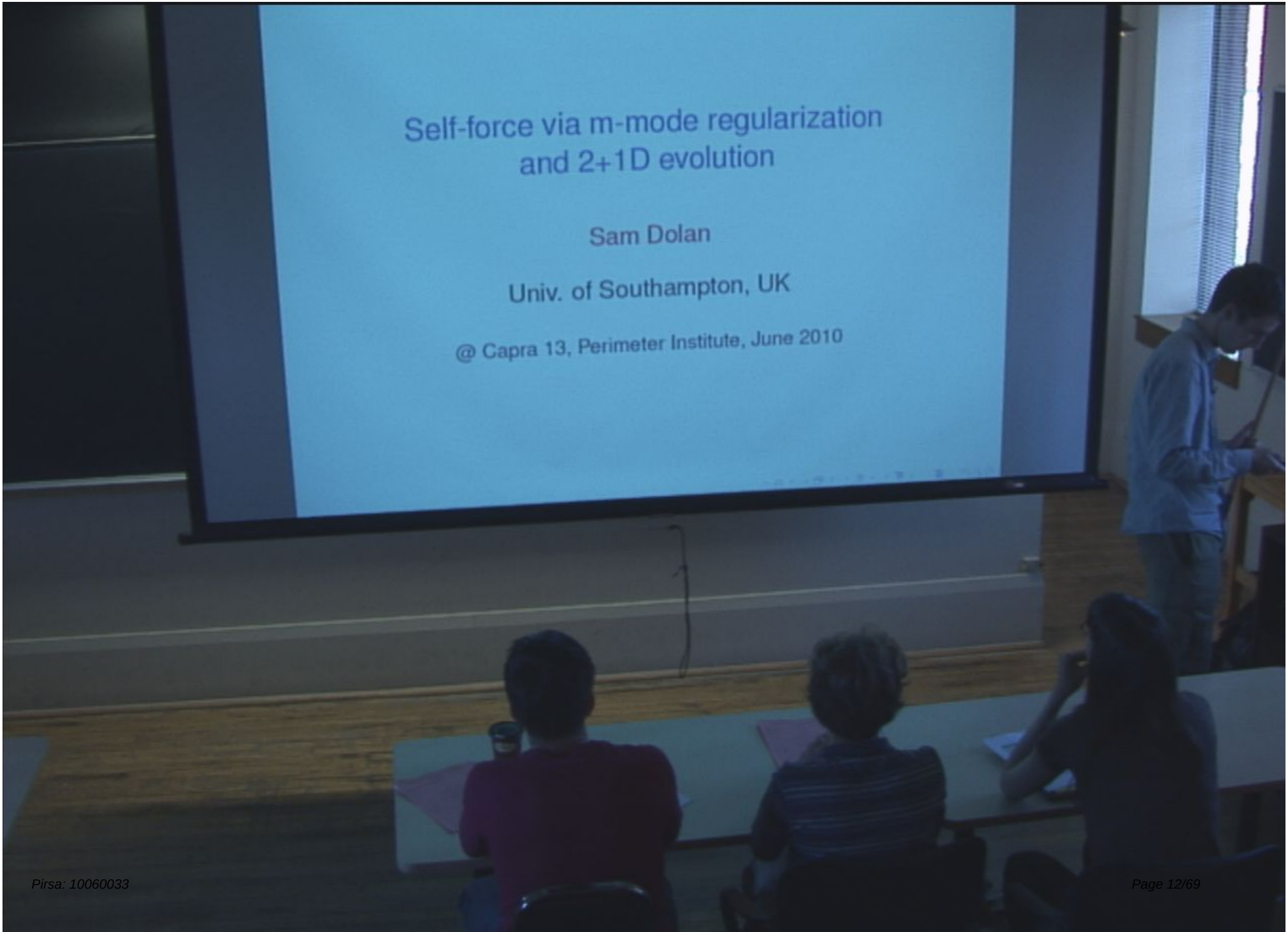
Self-force via m-mode regularization
and 2+1D evolution
Sam Dolan
Univ. of Southampton, UK
@ Capra 13, Perimeter Institute, June 2010

Self-force via m-mode regularization and 2+1D evolution

Sam Dolan

Univ. of Southampton, UK

@ Capra 13, Perimeter Institute, June 2010

Self-force via m-mode regularization and 2+1D evolution

Sam Dolan

Univ. of Southampton, UK

@ Capra 13, Perimeter Institute, June 2010

Self-force via m-mode regularization and 2+1D evolution

Sam Dolan

Univ. of Southampton, UK

@ Capra 13, Perimeter Institute, June 2010

Outline

1. Puncture Formulations
   - Detweiler-Whiting splitting (into R and S fields)
   - Order of puncture and smoothness of residual
   - m-mode convergence
2. Scalar SF for circular orbits on Schwarzschild
   - Puncture + Worldtube + m-mode scheme
   - Finite difference method in 2+1D
   - Results: 2nd, 3rd & 4th order punctures
3. Scalar SF for circular orbits on Kerr
   - Finite difference schemes
   - Numerical stability
   - Results and accuracy
4. Conclusions + Future Work

Outline

1. Puncture Formulations
   - Detweiler-Whiting splitting (into R and S fields)
   - Order of puncture and smoothness of residual
   - m-mode convergence
2. Scalar SF for circular orbits on Schwarzschild
   - Puncture + Worldtube + m-mode scheme
   - Finite difference method in 2+1D
   - Results: 2nd, 3rd & 4th order punctures
3. Scalar SF for circular orbits on Kerr
   - Finite difference schemes
   - Numerical stability
   - Results and accuracy
4. Conclusions + Future Work

Outline

1. Puncture Formulations
   - Detweiler-Whiting splitting (into R and S fields)
   - Order of puncture and smoothness of residual
   - m-mode convergence
2. Scalar SF for circular orbits on Schwarzschild
   - Puncture + Worldtube + m-mode scheme
   - Finite difference method in 2+1D
   - Results: 2nd, 3rd & 4th order punctures
3. Scalar SF for circular orbits on Kerr
   - Finite difference schemes
   - Numerical stability
   - Results and accuracy
4. Conclusions + Future Work

Outline

1. Puncture Formulations
   - Detweiler-Whiting splitting (into R and S fields)
   - Order of puncture and smoothness of residual
   - m-mode convergence
2. Scalar SF for circular orbits on Schwarzschild
   - Puncture + Worldtube + m-mode scheme
   - Finite difference method in 2+1D
   - Results: 2nd, 3rd & 4th order punctures
3. Scalar SF for circular orbits on Kerr
   - Finite difference schemes
   - Numerical stability
   - Results and accuracy
4. Conclusions + Future Work

Outline

1. Puncture Formulations
   - Detweiler-Whiting splitting (into R and S fields)
   - Order of puncture and smoothness of residual
   - m-mode convergence
2. Scalar SF for circular orbits on Schwarzschild
   - Puncture + Worldtube + m-mode scheme
   - Finite difference method in 2+1D
   - Results: 2nd, 3rd & 4th order punctures
3. Scalar SF for circular orbits on Kerr
   - Finite difference schemes
   - Numerical stability
   - Results and accuracy
4. Conclusions + Future Work

Outline

1. Puncture Formulations
   - Detweiler-Whiting splitting (into R and S fields)
   - Order of puncture and smoothness of residual
   - m-mode convergence
2. Scalar SF for circular orbits on Schwarzschild
   - Puncture + Worldtube + m-mode scheme
   - Finite difference method in 2+1D
   - Results: 2nd, 3rd & 4th order punctures
3. Scalar SF for circular orbits on Kerr
   - Finite difference schemes
   - Numerical stability
   - Results and accuracy
4. Conclusions + Future Work

Outline

1. Puncture Formulations
   - Detweiler-Whiting splitting (into R and S fields)
   - Order of puncture and smoothness of residual
   - m-mode convergence
2. Scalar SF for circular orbits on Schwarzschild
   - Puncture + Worldtube + m-mode scheme
   - Finite difference method in 2+1D
   - Results: 2nd, 3rd & 4th order punctures
3. Scalar SF for circular orbits on Kerr
   - Finite difference schemes
   - Numerical stability
   - Results and accuracy
4. Conclusions + Future Work

Detweiler-Whiting Formulation (I)

- Worldline γ described by $z(\tau)$
- Scalar field equation: $\Box\Phi(x) = S(x)$

$$S(x) = -4\pi q \int_\gamma (-g)^{1/2}\delta^4[x - z(\tau)]d\tau$$

- Self-force from radiative (R) field:

$$F_\mu^{(\text{self})} = \lim_{x\to z} \nabla_\mu \Phi^R$$

- Subtract singular (S) field: $\Phi^R \equiv \Phi - \Phi^S$
- S field from integral of Green function along worldline :

$$\Phi^S = \int_\gamma G^S(x, z(\tau))d\tau$$

Detweiler-Whiting Formulation (I)

- Worldline γ described by $z(\tau)$
- Scalar field equation: $\Box\Phi(x) = S(x)$

$$S(x) = -4\pi q \int_\gamma (-g)^{1/2}\delta^4[x - z(\tau)]d\tau$$

- Self-force from radiative (R) field:

$$F_\mu^{(\text{self})} = \lim_{x\to z} \nabla_\mu \Phi^R$$

- Subtract singular (S) field: $\Phi^R \equiv \Phi - \Phi^S$
- S field from integral of Green function along worldline :

$$\Phi^S = \int_\gamma G^S(x, z(\tau))d\tau$$

Detweiler-Whiting Formulation (I)

- Worldline γ described by $z(\tau)$
- Scalar field equation: $\Box\Phi(x) = S(x)$

$$S(x) = -4\pi q \int_\gamma (-g)^{1/2}\delta^4[x - z(\tau)]d\tau$$

- Self-force from radiative (R) field:

$$F_\mu^{(\text{self})} = \lim_{x\to z} \nabla_\mu \Phi^R$$

- Subtract singular (S) field: $\Phi^R \equiv \Phi - \Phi^S$
- S field from integral of Green function along worldline :

$$\Phi^S = \int_\gamma G^S(x, z(\tau))d\tau$$

Detweiler-Whiting Formulation (I)

- Worldline γ described by $z(\tau)$
- Scalar field equation: $\Box\Phi(x) = S(x)$

$$S(x) = -4\pi q \int_\gamma (-g)^{1/2}\delta^4[x - z(\tau)]d\tau$$

- Self-force from radiative (R) field:

$$F_\mu^{(\text{self})} = \lim_{x\to z} \nabla_\mu \Phi^R$$

- Subtract singular (S) field: $\Phi^R \equiv \Phi - \Phi^S$
- S field from integral of Green function along worldline :

$$\Phi^S = \int_\gamma G^S(x, z(\tau))d\tau$$

Detweiler-Whiting Formulation (I)

- Worldline γ described by $z(\tau)$
- Scalar field equation: $\Box\Phi(x) = S(x)$

$$S(x) = -4\pi q \int_\gamma (-g)^{1/2} \delta^4[x - z(\tau)]d\tau$$

- Self-force from radiative (R) field:

$$F_\mu^{(\text{self})} = \lim_{x \to z} \nabla_\mu \Phi^R$$

- Subtract singular (S) field: $\Phi^R \equiv \Phi - \Phi^S$
- S field from integral of Green function along worldline :

$$\Phi^S = \int_\gamma G^S(x, z(\tau))d\tau$$

Puncture Schemes

- Idea: Approximate the (S) field with a puncture field.
- U, V, σ in coordinate expansions $\delta x^\mu = x^\mu - z^\mu$
- Introduce puncture $\Phi_\mathcal{P}$ and residual $\Phi_\mathcal{R} = \Phi - \Phi_\mathcal{P}$
- Higher-order puncture $\Rightarrow$ better results.
- Meaning of order? Classify by "smoothness" of $\Phi_\mathcal{R}$
- Introduce scaling parameter λ : $\delta x^\mu = \lambda \delta \bar{x}^\mu$
- 1st order puncture: $\Phi^{(1)}_\mathcal{P} = q/|\epsilon|$

$$\epsilon^2 = \lambda^2 \left(g_{\mu\nu} + u_\mu u_\nu\right) \delta\bar{x}^\mu \delta\bar{x}^\nu$$

- $\Phi^{(1)}_\mathcal{R} \sim \mathcal{O}(\lambda/|\lambda|)$ i.e. discontinuous at worldline, C^{-1}

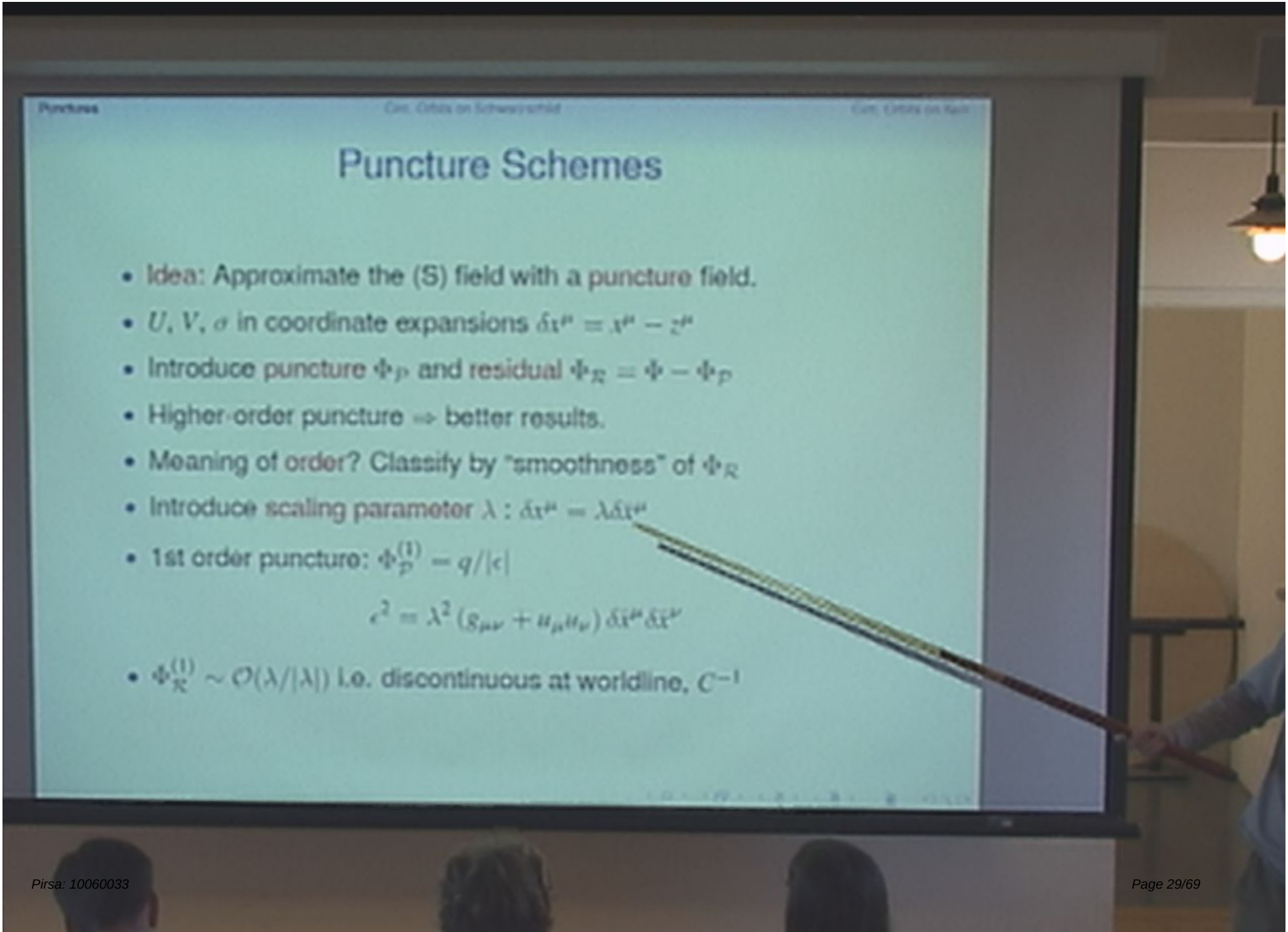
Puncture Schemes
• Idea: Approximate the (S) field with a puncture field.
• U, V, σ in coordinate expansions $\delta x^\mu = x^\mu - z^\mu$
• Introduce puncture Φ_P and residual $\Phi_R = \Phi - \Phi_P$
• Higher-order puncture ⇒ better results.
• Meaning of order? Classify by "smoothness" of Φ_R
• Introduce scaling parameter λ : $\delta x^\mu = \lambda \delta x^\mu$
• 1st order puncture: $\Phi_P^{(1)} = q/|\epsilon|$
$$\epsilon^2 = \lambda^2 \left(g_{\mu\nu} + u_\mu u_\nu\right) \delta x^\mu \delta x^\nu$$
• $\Phi_R^{(1)} \sim \mathcal{O}(\lambda/|\lambda|)$ i.e. discontinuous at worldline, C^{-1}

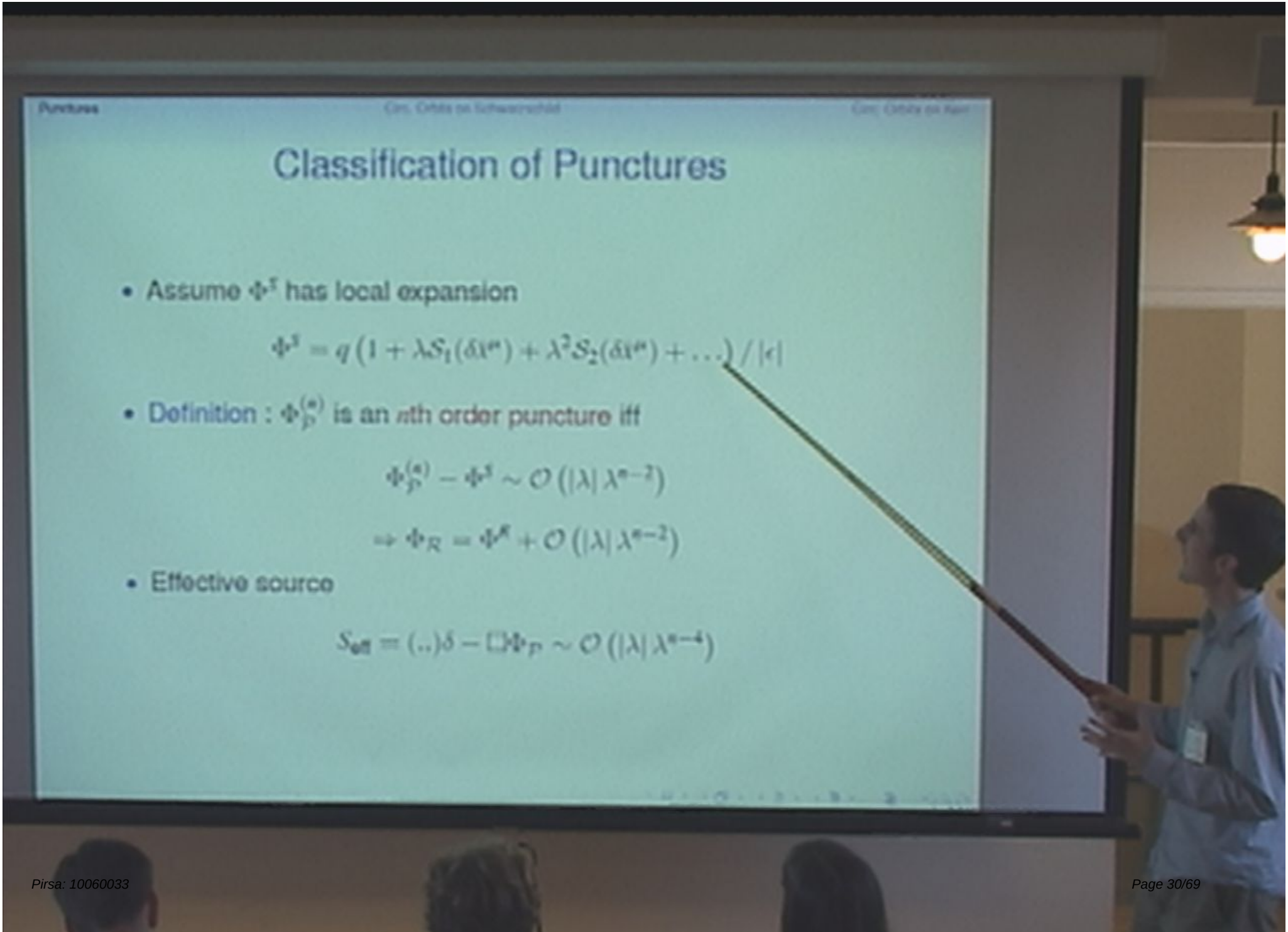
Punctures
Circ. Orbits on Schwarzschild
Circ. Orbits on Kerr
Classification of Punctures
• Assume Φ^S has local expansion
$$\Phi^S = q\left(1 + \lambda S_1(\delta x^a) + \lambda^2 S_2(\delta x^a) + \ldots\right)/|\epsilon|$$
• Definition : $\Phi_P^{(n)}$ is an nth order puncture iff
$$\Phi_P^{(n)} - \Phi^S \sim \mathcal{O}\left(|\lambda|\,\lambda^{n-2}\right)$$
$$\Rightarrow \Phi_R = \Phi^R + \mathcal{O}\left(|\lambda|\,\lambda^{n-2}\right)$$
• Effective source
$$S_{\text{eff}} = (..)\delta - \Box\Phi_P \sim \mathcal{O}\left(|\lambda|\,\lambda^{n-4}\right)$$

Classification of Punctures

- Assume Φ^S has local expansion

$$\Phi^S = q\left(1 + \lambda \mathcal{S}_1(\delta\bar{x}^\mu) + \lambda^2 \mathcal{S}_2(\delta\bar{x}^\mu) + \ldots\right) / |\epsilon|$$

- Definition : $\Phi^{(n)}_{\mathcal{P}}$ is an nth order puncture iff

$$\Phi^{(n)}_{\mathcal{P}} - \Phi^S \sim \mathcal{O}\left(|\lambda|\,\lambda^{n-2}\right)$$

$$\Rightarrow \Phi_{\mathcal{R}} = \Phi^R + \mathcal{O}\left(|\lambda|\,\lambda^{n-2}\right)$$

- Effective source

$$S_{\text{eff}} = (..)\delta - \Box\Phi_{\mathcal{P}} \sim \mathcal{O}\left(|\lambda|\,\lambda^{n-4}\right)$$

Classification of Punctures

- Assume Φ^S has local expansion

$$\Phi^S = q\left(1 + \lambda \mathcal{S}_1(\delta\bar{x}^\mu) + \lambda^2 \mathcal{S}_2(\delta\bar{x}^\mu) + \ldots\right) / |\epsilon|$$

- Definition : $\Phi^{(n)}_{\mathcal{P}}$ is an nth order puncture iff

$$\Phi^{(n)}_{\mathcal{P}} - \Phi^S \sim \mathcal{O}\left(|\lambda|\,\lambda^{n-2}\right)$$

$$\Rightarrow \Phi_{\mathcal{R}} = \Phi^R + \mathcal{O}\left(|\lambda|\,\lambda^{n-2}\right)$$

- Effective source

$$S_{\text{eff}} = (..)\delta - \Box\Phi_{\mathcal{P}} \sim \mathcal{O}\left(|\lambda|\,\lambda^{n-4}\right)$$

Classification of Punctures

order	$\Phi_{\mathcal{R}}$	C	$S_{\text{eff}} = -\Box\Phi_{\mathcal{P}}$	
1st	$\lambda/\lvert\lambda\rvert$	C^{-1}	$1/\lvert\lambda\rvert\lambda$	e.g. Barack & Golbourn (2007)
2nd	$\lvert\lambda\rvert$	C^{0}	$1/\lvert\lambda\rvert$	e.g. B, G & Sago (2007)
3rd	$\lvert\lambda\rvert\,\lambda$	C^{1}	$\lambda/\lvert\lambda\rvert$	Wardell (2010)
4th	$\lvert\lambda\rvert\,\lambda^2$	C^{2}	$\lvert\lambda\rvert$	Wardell (2010)

4th-order Effective Source

- 4th order residual field is $\mathcal{O}(\lambda^2|\lambda|)$.
- Source is continuous $\mathcal{O}(|\lambda|)$ on worldline

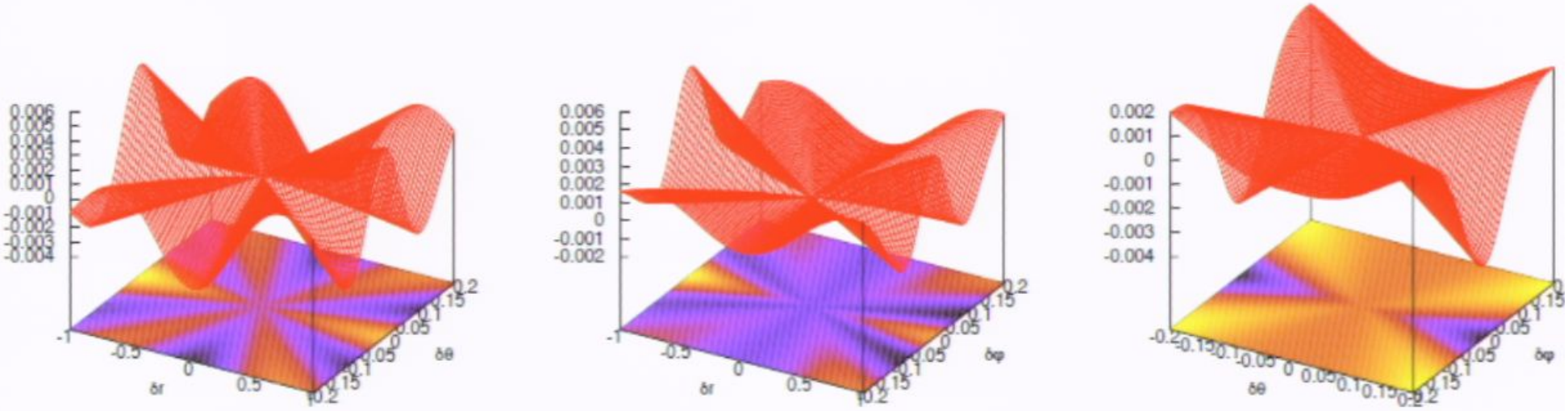

Figure: Source S_{eff} obtained from fourth-order puncture field $\Phi_{\mathcal{P}}$ (with thanks to B. Wardell).

m-mode Scheme

- Decompose field + source in azimuthal modes, e.g.

$$\Phi_{\mathcal{R}} = \sum_{m=-\infty}^{\infty} \Phi^m_{\mathcal{R}} e^{im\varphi} \quad \Leftrightarrow \quad \Phi^m_{\mathcal{R}} = \frac{1}{2\pi} \int_{-\pi}^{\pi} \Phi_{\mathcal{R}}\, e^{-im\varphi} d\varphi$$

- Smoothness of $\Phi_{\mathcal{R}}$ $\Leftrightarrow$ Convergence of mode sum

m-mode Scheme

- Decompose field + source in azimuthal modes, e.g.

$$\Phi_{\mathcal{R}} = \sum_{m=-\infty}^{\infty} \Phi^m_{\mathcal{R}} e^{im\varphi} \quad \Leftrightarrow \quad \Phi^m_{\mathcal{R}} = \frac{1}{2\pi} \int_{-\pi}^{\pi} \Phi_{\mathcal{R}}\, e^{-im\varphi} d\varphi$$

- Smoothness of $\Phi_{\mathcal{R}}$ $\Leftrightarrow$ Convergence of mode sum
- Example: Consider 1D toy model,

$$f(\lambda) = \left(\alpha\lambda + \beta\lambda^2 + \gamma\lambda^3 + \ldots\right)/|\lambda|$$

- Fourier reconstruction :

$$\sum_{m=-\infty}^{\infty} f^m = \text{const.} + \alpha A \sum_{\text{odd}} \frac{\sin(m\lambda)}{m} + \beta B \sum_{\text{even}} \frac{\cos(m\lambda)}{m^2} + \gamma C \sum_{\text{odd}} \frac{\sin(m\lambda)}{m^3}$$

m-mode Convergence

order	$\Phi_{\mathcal{R}}$	C	S_{eff}	field Φ^m	s.f. $\partial_r \Phi^m$
1	$\lambda/\lvert\lambda\rvert$	C^{-1}	$1/\lambda^2$	m^{-2}	—
2	$\lvert\lambda\rvert$	C^0	$1/\lvert\lambda\rvert$	m^{-2}	m^{-2}
3	$\lvert\lambda\rvert\,\lambda$	C^1	$\lambda/\lvert\lambda\rvert$	m^{-4}	m^{-2}
4	$\lvert\lambda\rvert\,\lambda^2$	C^2	$\lvert\lambda\rvert$	m^{-4}	m^{-4}

SF for circular orbits on Schwarzschild

- Successful implementation combines many ingredients:
  1. Puncture (2nd, 3rd, or 4th order)
  2. Decomposition in $e^{im\phi}$
  3. World-tube formulation
  4. Finite Difference method
  5. multiple 2+1D simulations
  6. Extrapolation to infinite resolution
  7. Mode sums

- Compute SF from mode sums [where $\tilde{\Phi}^{(m)} = e^{im\varphi}\Phi^{(m)}$]:

$$\text{dissipative} : \quad F_a = -2q \operatorname{Im} \sum_{m=1} m\tilde{\Phi}^{(m)}$$

$$\text{conservative} : \quad F_r = \partial_r \Phi^{(m=0)} + 2 \operatorname{Re} \sum_{m=1} \partial_r \tilde{\Phi}^{(m)}$$

SF for circular orbits on Schwarzschild

- Successful implementation combines many ingredients:
  1. Puncture (2nd, 3rd, or 4th order)
  2. Decomposition in $e^{im\phi}$
  3. World-tube formulation
  4. Finite Difference method
  5. multiple 2+1D simulations
  6. Extrapolation to infinite resolution
  7. Mode sums

- Compute SF from mode sums [where $\tilde{\Phi}^{(m)} = e^{im\omega t}\Phi^{(m)}$]:

$$\text{dissipative}: \quad F_\phi = -2\omega\, \text{Im} \sum_{m=1}^{\infty} m\tilde{\Phi}^{(m)}$$

$$\text{conservative}: \quad F_r = \partial_r \Phi^{(m=0)} + 2\,\text{Re} \sum_{m=1}^{\infty} \partial_r \tilde{\Phi}^{(m)}$$

World-tube Construction

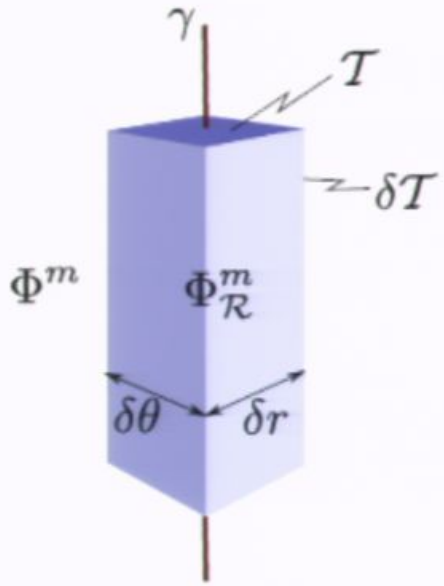

- Worldtube $\mathcal{T}$ of fixed dimensions δr, $\delta\theta$
- Outside: $\Box_m \Phi^m = 0$
- Inside: $\Box_m \Phi^m_{\mathcal{R}} = S^m_{\text{eff}}$, where

$$S^m_{\text{eff}} = \frac{1}{2\pi} \int_{-\pi}^{\pi} e^{-im\varphi} \left(-\Box \Phi_{\mathcal{P}}\right) d\varphi$$

- On boundary $\delta\mathcal{T}$: $\Phi^m_{\mathcal{P}} = \Phi^m - \Phi^m_{\mathcal{R}}$

2+1D Grid

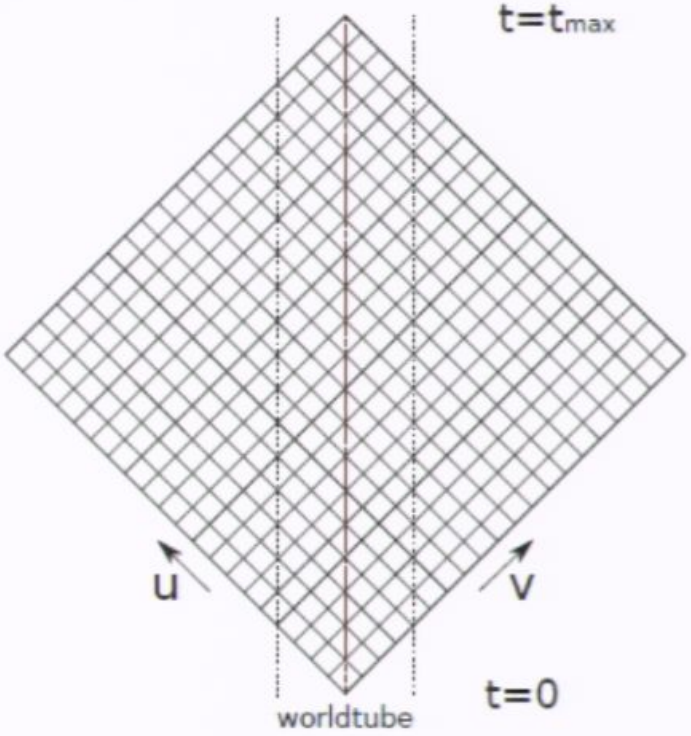

Figure: Diamond Grid in u, v.

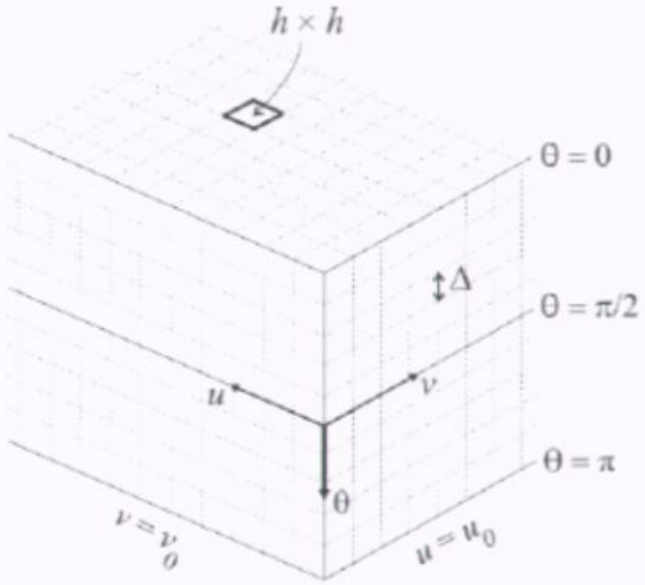

Figure: Full 2+1D Grid in u, v, θ.

- Use null coords $u = t - r_*, \quad v = t + r_*$
- Evolve Schw. wave equation for $\Psi^m = r\Phi^m$:

$$\Psi^m_{,uv} - \frac{f}{4r^2}\left[\Psi^m_{,\theta\theta} + \cot\theta\Psi^m_{,\theta} - \left(2M/r + m^2\csc^2\theta\right)\Psi^m\right] = -\frac{rf(r)}{4}S^m$$

2nd Order Finite Difference Scheme

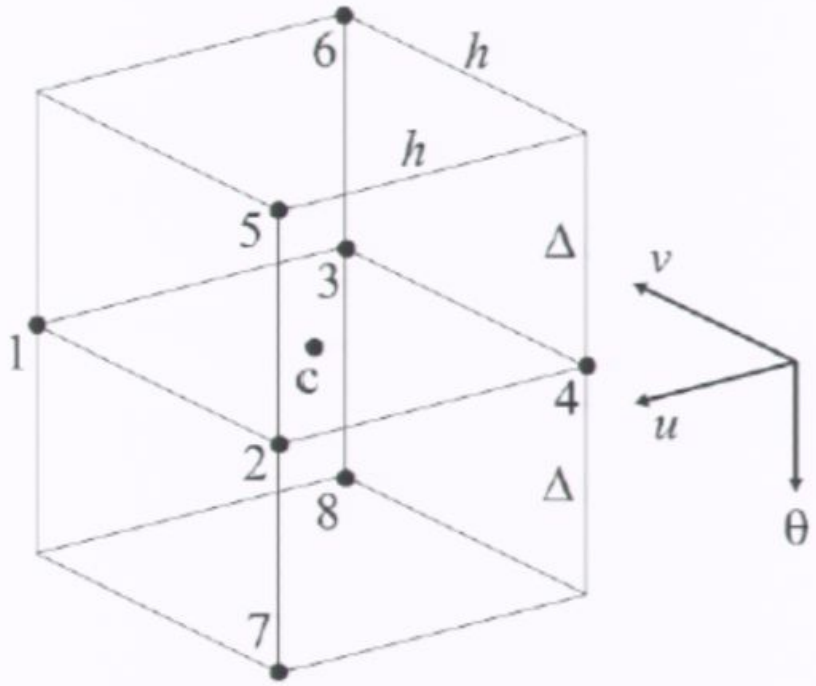

FD scheme of
Barack & Golbourn '07

$$\Psi_1^m = \Psi_2^m + \Psi_3^m - \Psi_4^m + \frac{h^2 f}{8r^2}\left[\frac{\Psi_5^m + \Psi_6^m + \Psi_7^m + \Psi_8^m - 2\Psi_2 - 2\Psi_3}{\Delta^2} + \cot\theta \frac{\Psi_5^m + \Psi_6^m - \Psi_7^m - \Psi_8^m}{2\Delta}\right] - \frac{h^2 f}{8r^2}\left(2M/r + m^2 \csc^2\theta\right)\left(\Psi_2^m + \Psi_3^m\right) + \mathcal{O}\left(h^2\Delta^2, h^4\right)$$

Numerical Instability

- Numerical instability can arise near poles
- Von Neumann analysis $\Rightarrow$ stability condition on ratio of grid spacings $h = \Delta u = \Delta v$ and $\Delta\theta$,

$$\frac{\Delta\theta}{h} \geq \frac{1}{2} \max\left(r^{-1} f^{1/2}\right) \sqrt{1 + \frac{m^2}{4}}$$

- More restrictive than Courant, c.f. $\frac{\Delta\theta}{h} \geq \max\left(r^{-1} f^{1/2}\right)$
- Mitigate by moving polar boundary points for high-m modes, using asymptotic behaviour of modes,

$$\Psi^m(\theta \approx 0, \pi) \sim \sin^m(\theta)$$

Extrapolation to Infinite Grid Resolution

1. Extract field along worldline

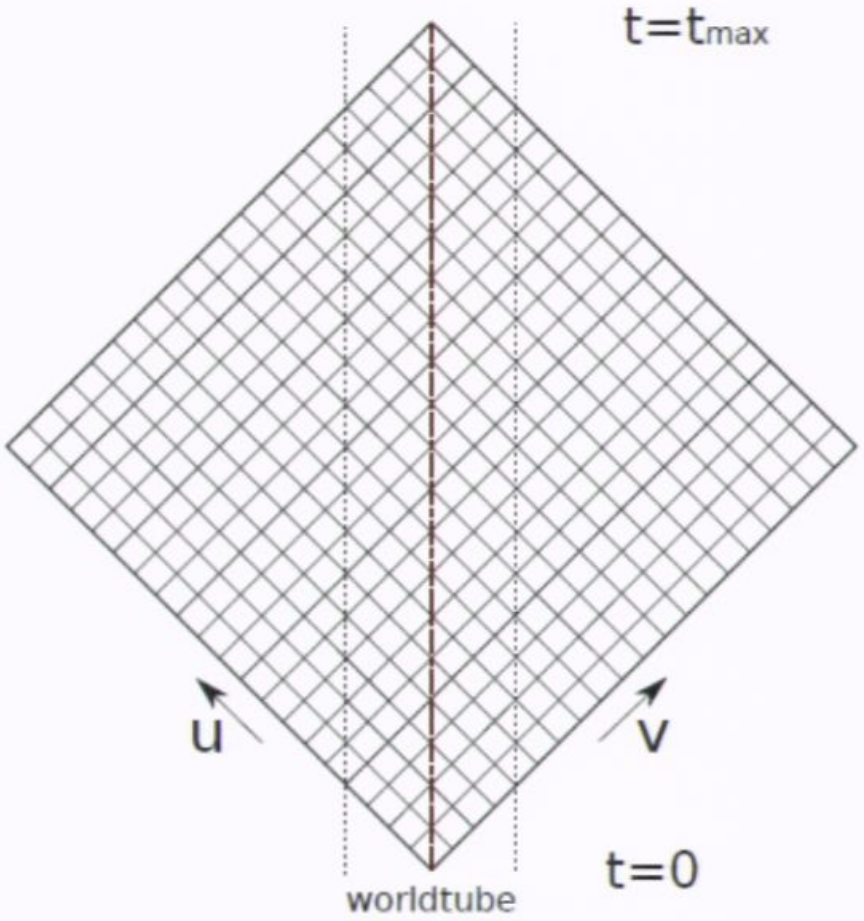

- Extract residual field $\Phi^m_{\mathcal{R}}$ (and derivs) along centre of diamond at

Extrapolation to Infinite Grid Resolution

2. Plot field $\Phi^m_{\mathcal{R}}$ as a function of time

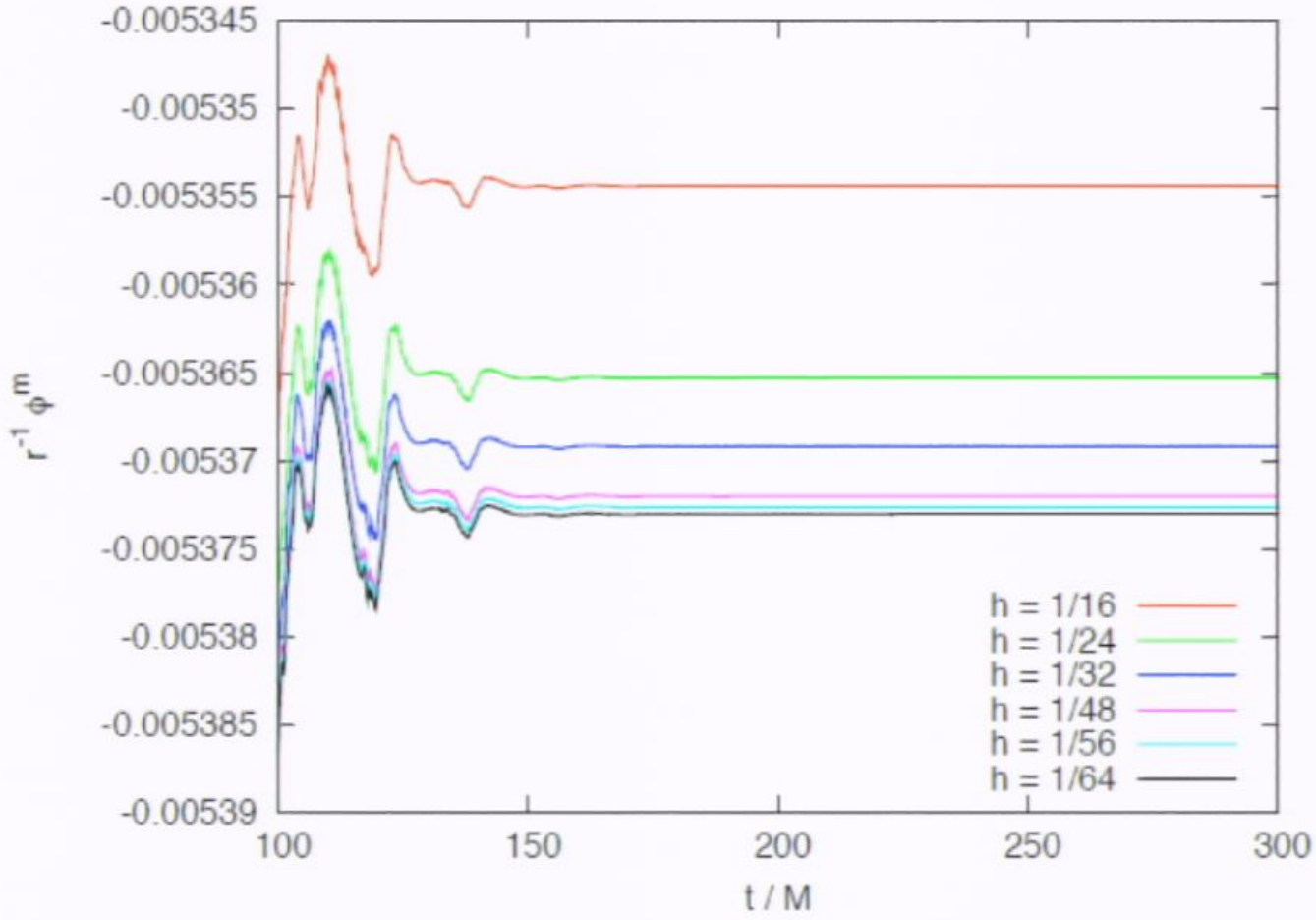

- Field depends on grid resolution h.

Extrapolation to Infinite Grid Resolution

3. Extrapolate field $\Phi^m_{\mathcal{R}}(t_{\max})$ as a function of grid resolution

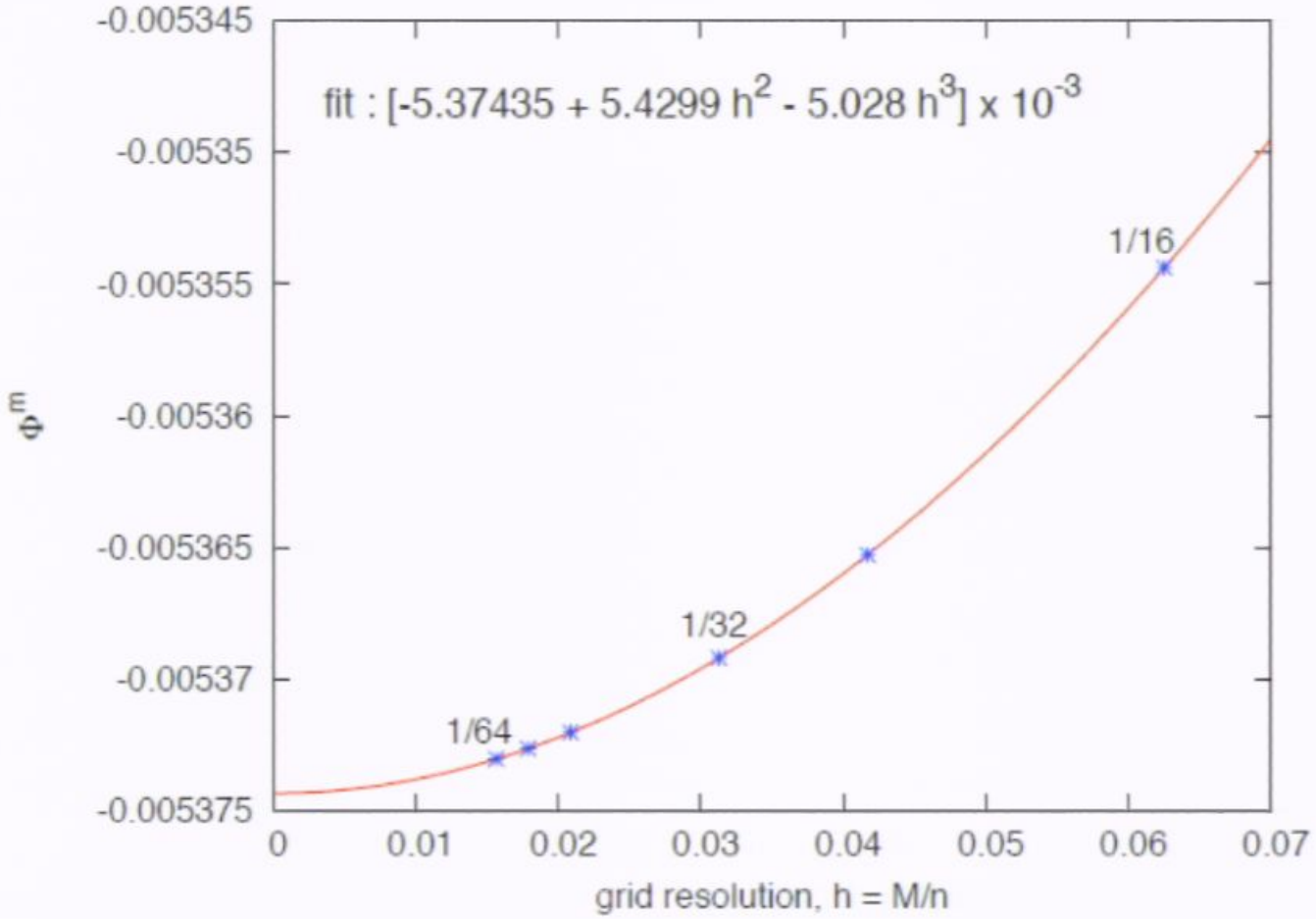

- 2nd order FD method $\Rightarrow$ Quadratic convergence $\propto h^2$

Extrapolation to Infinite Grid Resolution

2. Plot field $\Phi^m_{\mathcal{R}}$ as a function of time

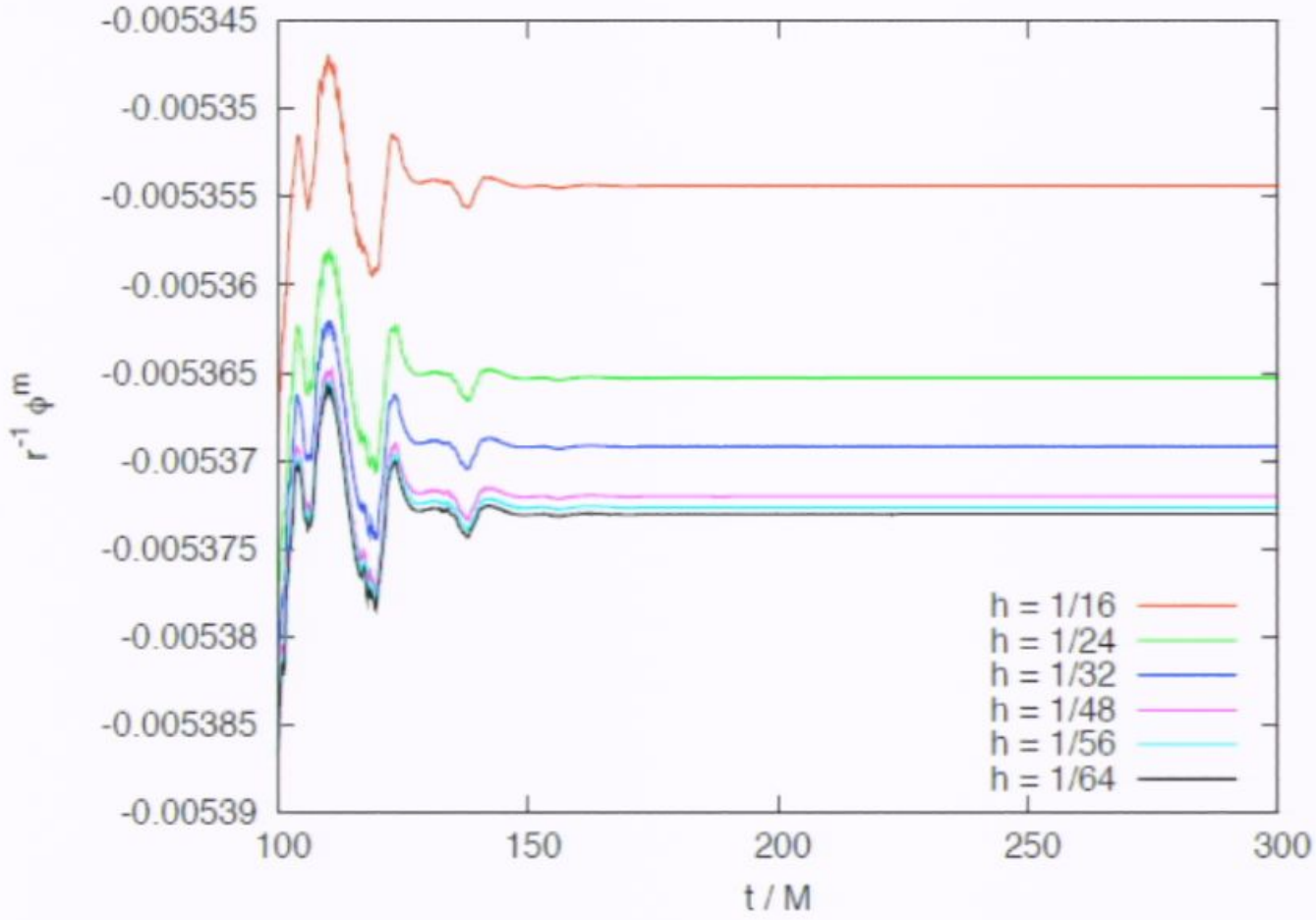

- Field depends on grid resolution h.

Extrapolation to Infinite Grid Resolution

3. Extrapolate field $\Phi^m_{\mathcal{R}}(t_{\max})$ as a function of grid resolution

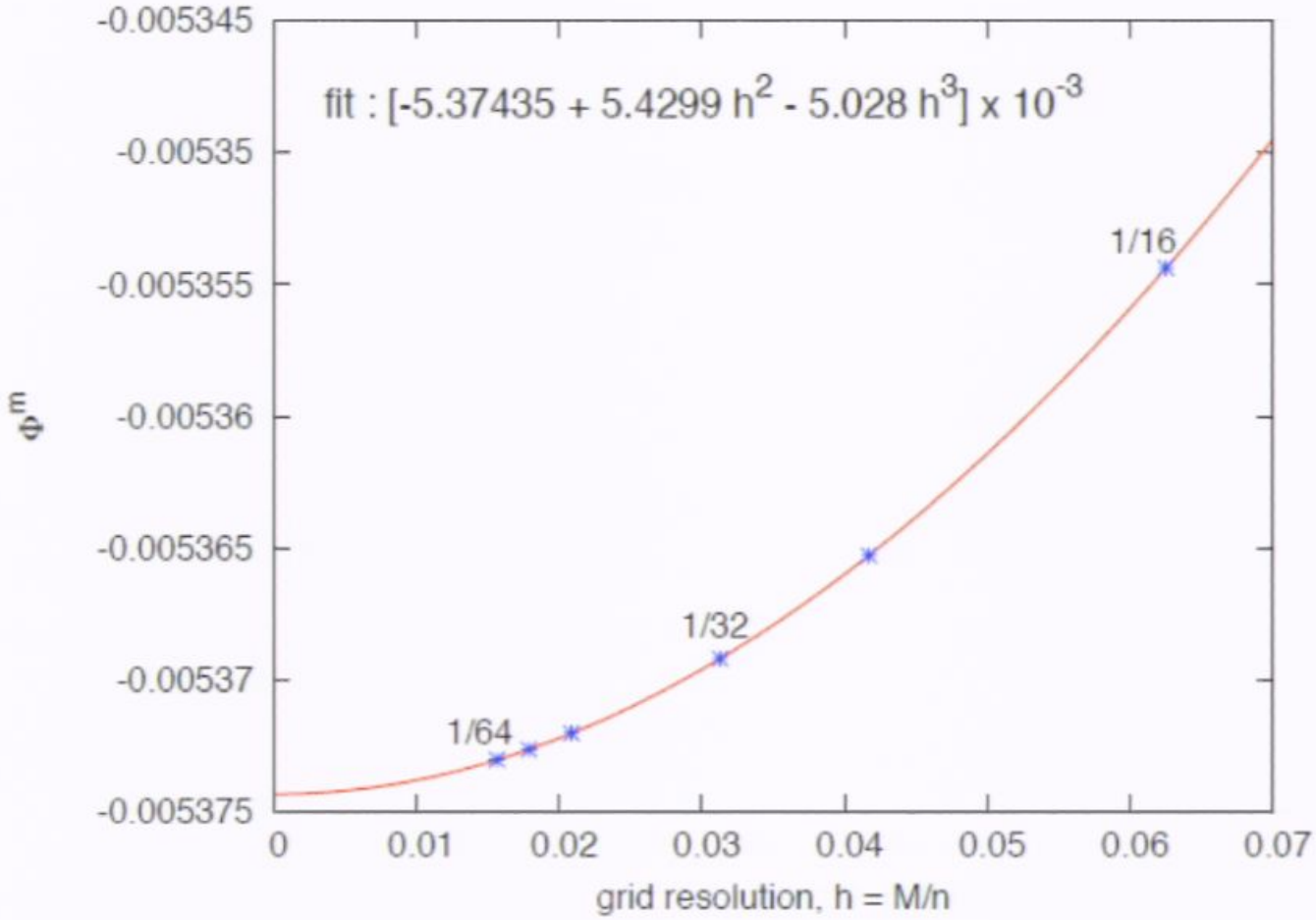

- 2nd order FD method $\Rightarrow$ Quadratic convergence $\propto h^2$

Sum over Modes : F_ϕ (dissipative)

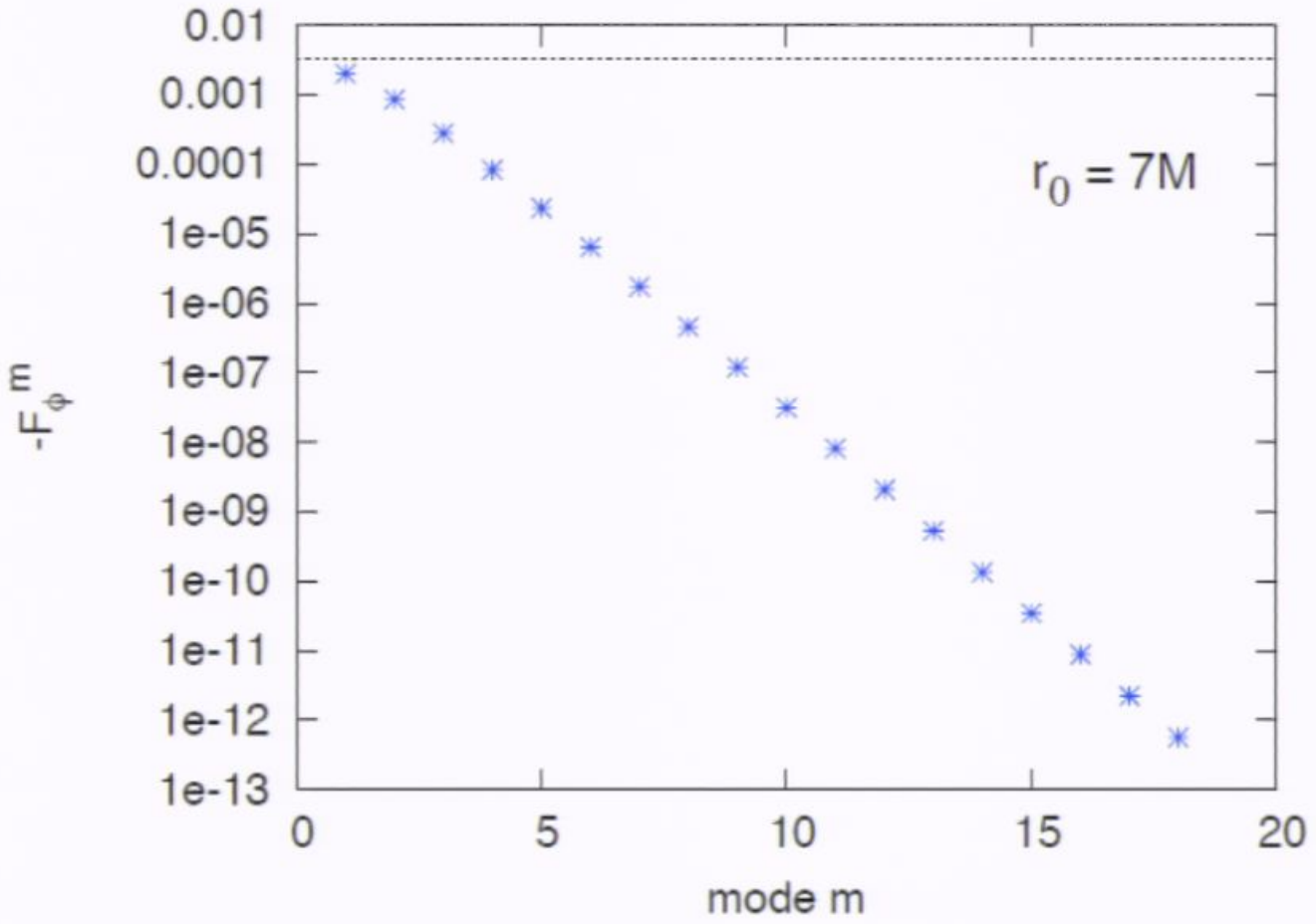

- Exponential convergence with m

Sum over Modes : F_r (conservative)

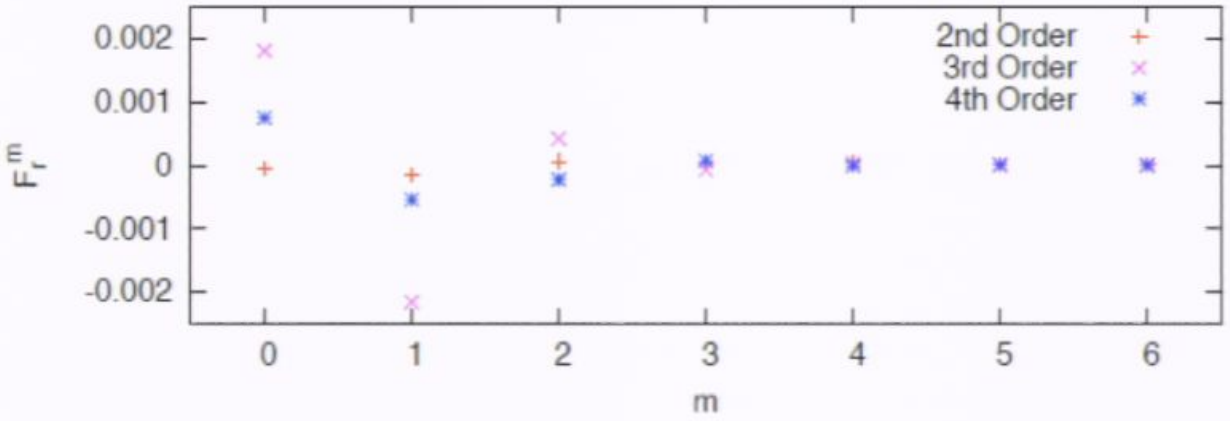

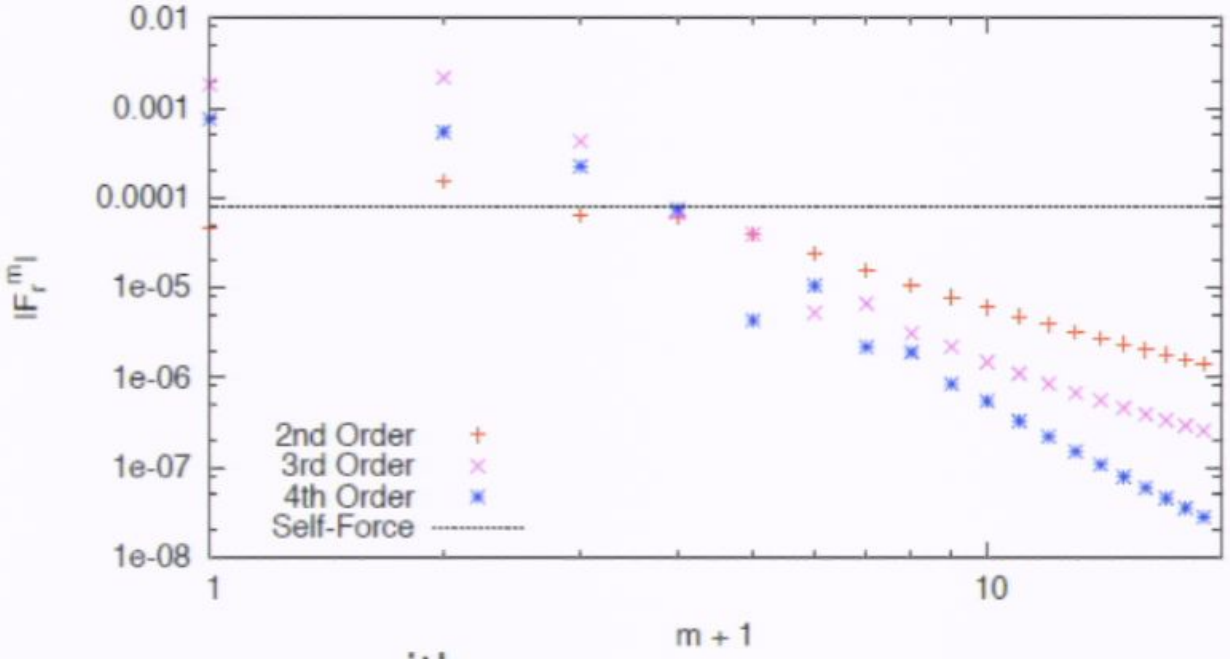

Power-law convergence with m:

- 2nd and 3rd order puncture $\Rightarrow m^{-2}$

F_r : Results from 2nd, 3rd, 4th Order Punctures

Example: Schw. at $r_0 = 7M$

order	F_r^m fit model	$\sum_m F_r^m$	error	tail ($m > 15$)
2	$\frac{A}{m^2} + \frac{B}{m^3} + \frac{C}{m^4}$	7.857e-5	$\lesssim 1\%$	31%
3	$\frac{A}{m^2} + \frac{B}{m^3} + \frac{C}{m^4}$	7.860e-5	$\lesssim 0.2\%$	5.4%
4	$\frac{A}{m^4} + \frac{B}{m^5} + \frac{C}{m^6}$	7.8506e-5	$\lesssim 0.05\%$	0.2%
∞	(freq. domain)	7.850679e-5		

Sum over Modes : F_r (conservative)

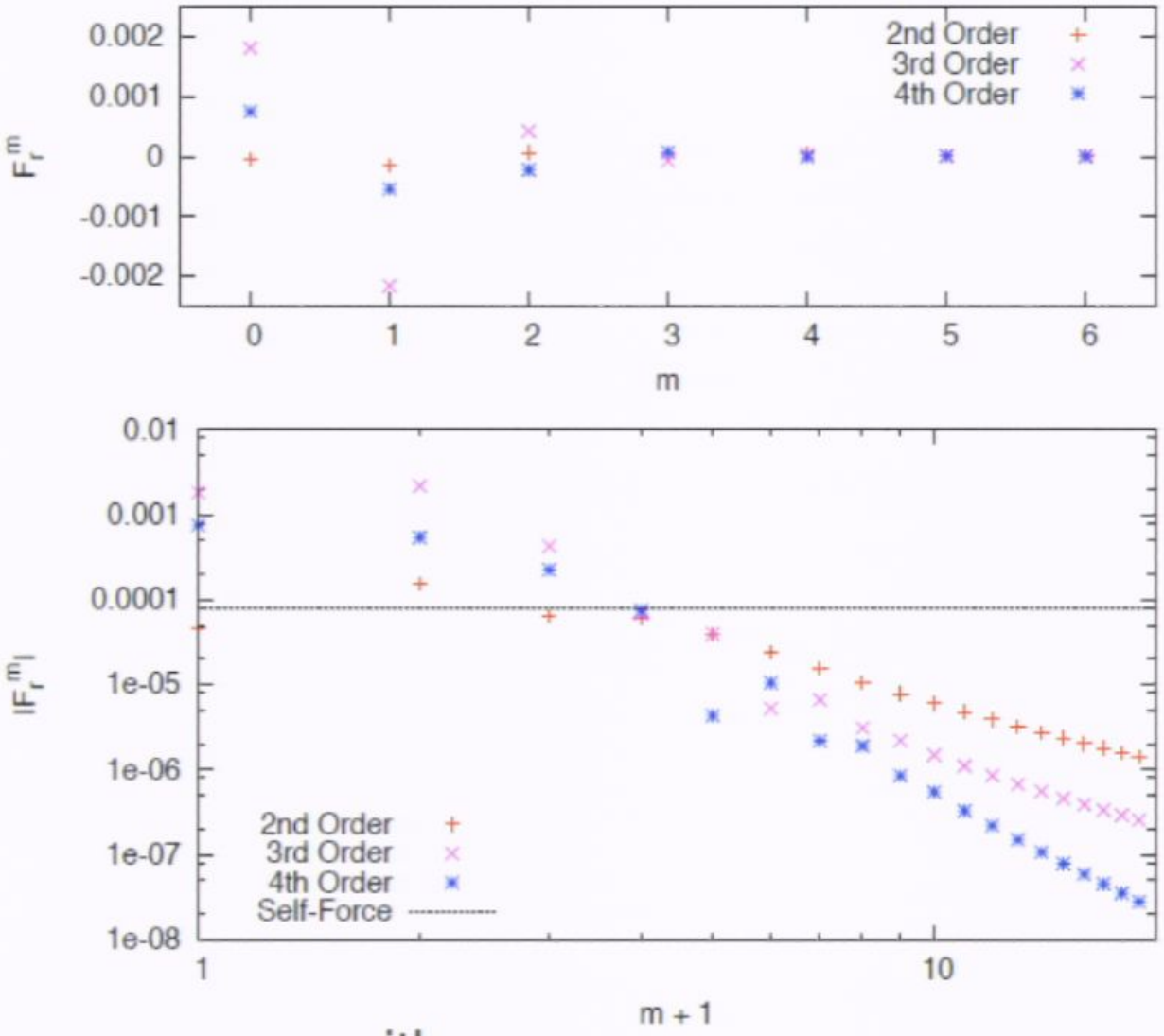

Power-law convergence with m:

- 2nd and 3rd order puncture $\Rightarrow m^{-2}$

F_r : Results from 2nd, 3rd, 4th Order Punctures

Example: Schw. at $r_0 = 7M$

order	F_r^m fit model	$\sum_m F_r^m$	error	tail ($m > 15$)
2	$\frac{A}{m^2} + \frac{B}{m^3} + \frac{C}{m^4}$	7.857e-5	$\lesssim 1\%$	31%
3	$\frac{A}{m^2} + \frac{B}{m^3} + \frac{C}{m^4}$	7.860e-5	$\lesssim 0.2\%$	5.4%
4	$\frac{A}{m^4} + \frac{B}{m^5} + \frac{C}{m^6}$	7.8506e-5	$\lesssim 0.05\%$	0.2%
∞	(freq. domain)	7.850679e-5		

Schw. Results : F_ϕ (dissipative)

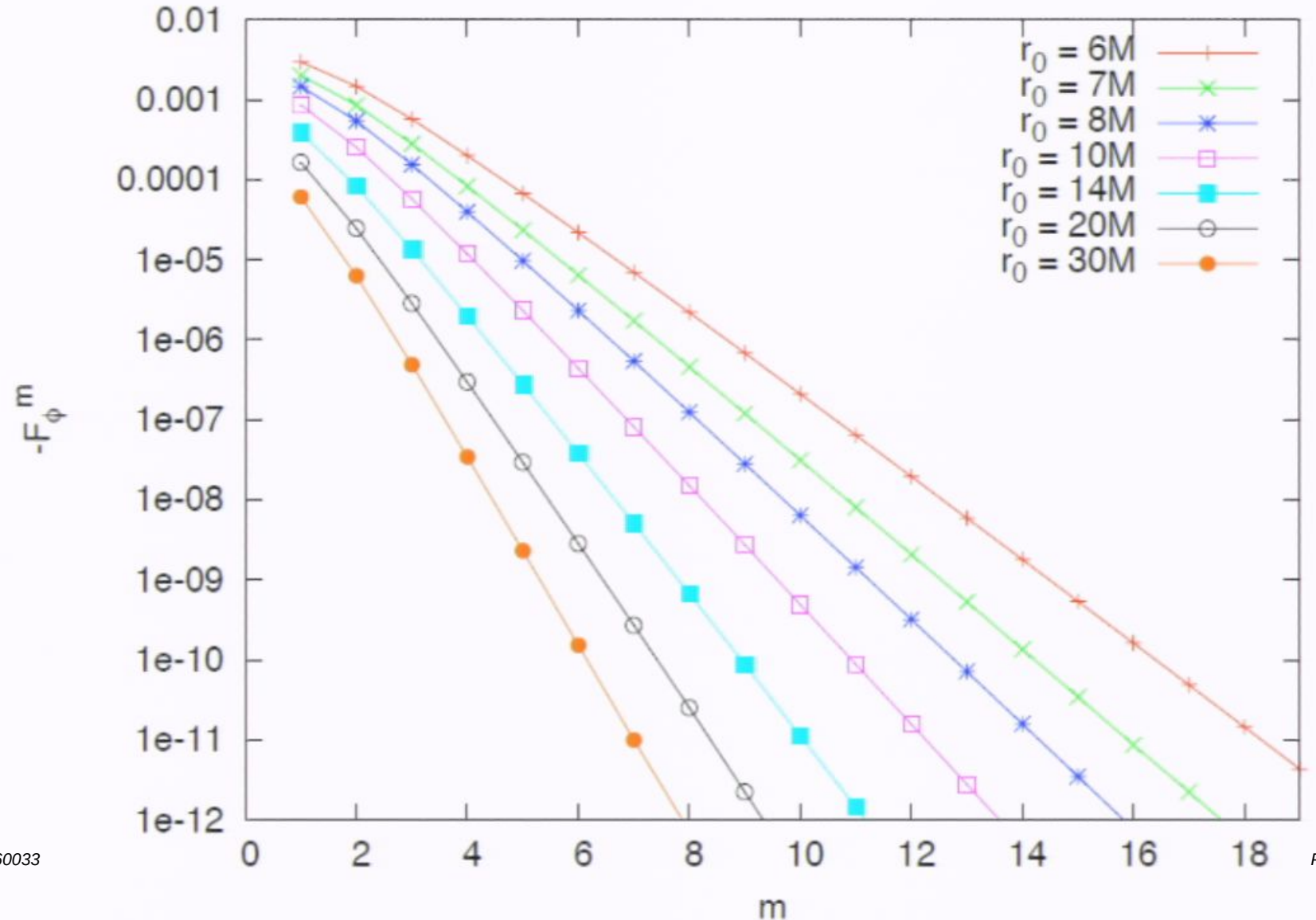

Schw. Results : F_ϕ (dissipative)

r_0	2+1D	Freq. Domain	error
6M	-5.304228e-3	-5.304232e-3	6.2e-5 %
7M	-3.273130e-3	-3.273123e-3	2.2e-4 %
8M	-2.211148e-3	-2.211161e-3	5.9e-4 %
10M	-1.185948e-3	-1.185926e-3	1.9e-3 %
14M	-4.838394e-4	-4.838493e-4	2.0e-3 %
20M	-1.926459e-4	-1.924442e-4	0.1 %

Schw. Results : F_r (conservative)

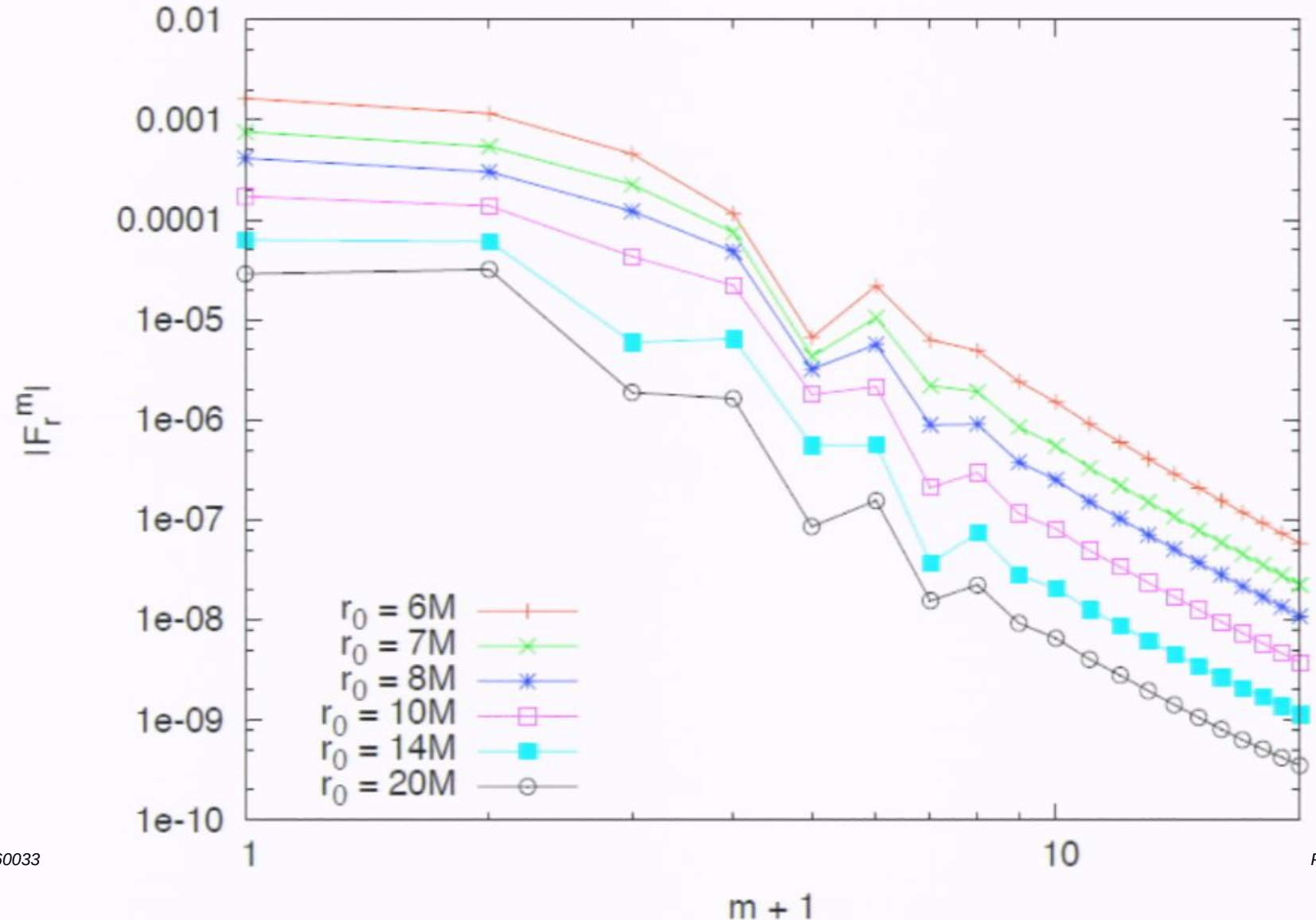

Schw. Results : F_r (conservative)

r_0	2+1D	Freq. Domain	error
6M	1.67736e-4	1.67728e-4	4.7e-3 %
7M	7.85072e-5	7.85068e-5	5.0e-4 %
8M	4.08283e-5	4.08250e-5	8.1e-3 %
10M	1.37987e-5	1.37845e-5	0.10 %
14M	2.73492e-6	2.72008e-6	0.54 %
20M	5.38309e-7	4.93790e-7	9.0 %

Schw. Results : F_ϕ (dissipative)

r_0	2+1D	Freq. Domain	error
6M	-5.304228e-3	-5.304232e-3	6.2e-5 %
7M	-3.273130e-3	-3.273123e-3	2.2e-4 %
8M	-2.211148e-3	-2.211161e-3	5.9e-4 %
10M	-1.185948e-3	-1.185926e-3	1.9e-3 %
14M	-4.838394e-4	-4.838493e-4	2.0e-3 %
20M	-1.926459e-4	-1.924442e-4	0.1 %

Schw. Results : F_r (conservative)

r_0	2+1D	Freq. Domain	error
6M	1.67736e-4	1.67728e-4	4.7e-3 %
7M	7.85072e-5	7.85068e-5	5.0e-4 %
8M	4.08283e-5	4.08250e-5	8.1e-3 %
10M	1.37987e-5	1.37845e-5	0.10 %
14M	2.73492e-6	2.72008e-6	0.54 %
20M	5.38309e-7	4.93790e-7	9.0 %

Sources of Error

Well Modelled :

- Source error (delicate cancellations in $\Box\Phi_{\mathcal{P}}$).
- Grid Resolution error ($h \to 0$)
- World-tube error
- m-mode tail-fitting error

Unmodelled (at present):

- Relaxation time error

Relaxation Time Error

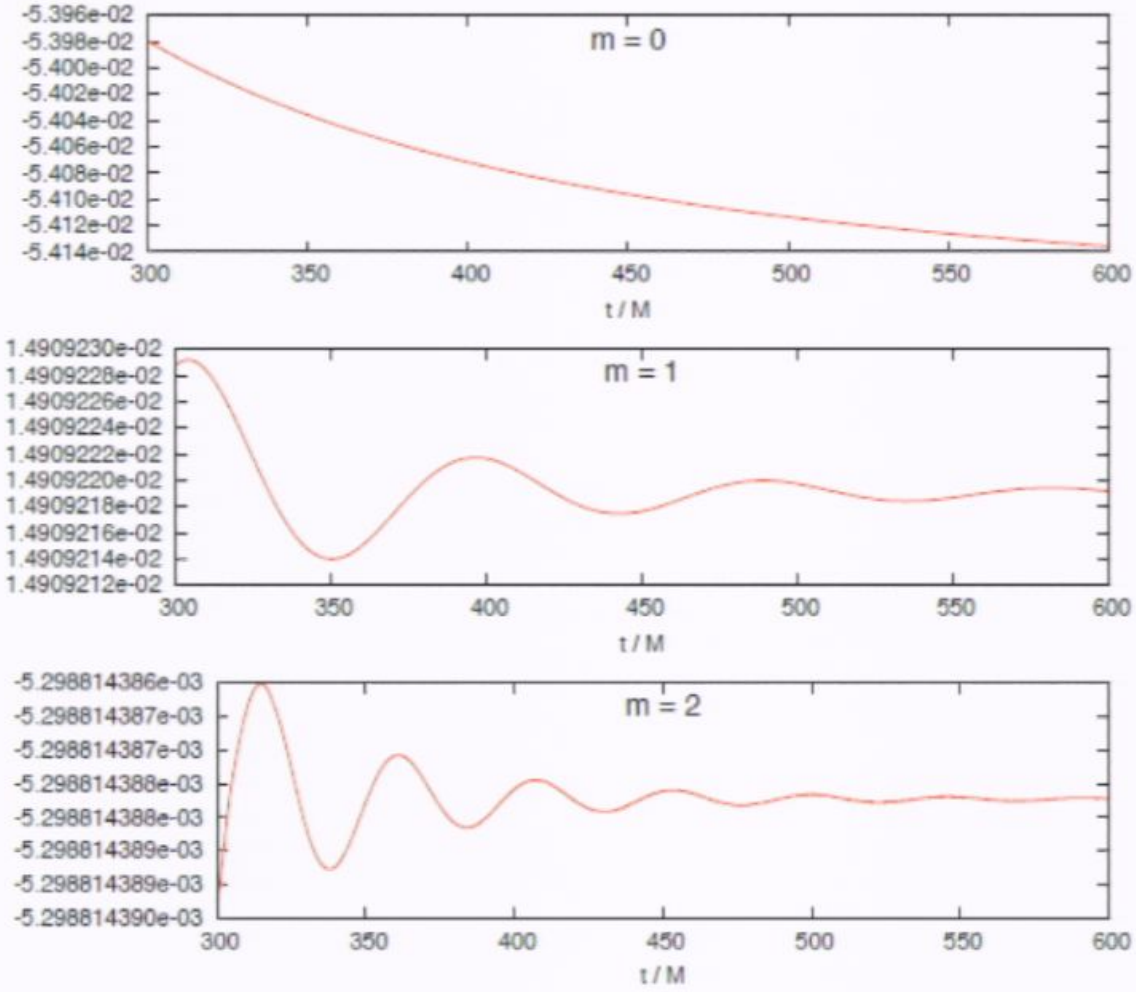

- Simulation must run for sufficiently long (t_{max}) that steady-state is reached.

SF for circular orbits on Kerr

- The first results for circular orbits on Kerr (frequency-domain) were presented by N. Warburton at Capra 12.
  - Parameters a and r_0.
  - Boyer-Lindquist coords. and $d\tilde{\phi} = d\phi - a/\Delta dr$
  - Kerr wave equation ($\Psi = \Psi^{\omega m}/r$, $\Delta = r^2 - 2Mr + a^2$):

$$\frac{\partial^2\Psi}{\partial r^2} - \frac{(r^2+a^2)^2}{\Sigma^2}\frac{\partial^2\Psi}{\partial t^2} + \frac{+4iamMr}{\Sigma^2}\frac{\partial\Psi}{\partial t} + \left[\frac{2a^2\Delta}{r\Sigma^2} - \frac{2iam(r^2+a^2)}{\Sigma^2}\right]\frac{\partial\Psi}{\partial r}$$

$$- \frac{\Delta}{\Sigma^2}\left[\frac{\partial^2}{\partial\theta^2} + \cot\theta\frac{\partial}{\partial\theta} - \frac{m^2}{\sin^2\theta} + r\left(\frac{\Delta}{r^2}\right)' - \frac{2iam}{r}\right]\Psi = 0$$

  - where

$$\Sigma^2 \equiv (r^2+a^2)^2 - a^2\Delta\sin^2\theta$$

SF for circular orbits on Kerr

- The first results for circular orbits on Kerr (frequency-domain) were presented by N. Warburton at Capra 12.
- Parameters a and r_0.
- Boyer-Lindquist coords, and $d\tilde{\phi} = d\phi + a/\Delta dr$
- Kerr wave equation ($\Psi = \Phi^m/r$, $\Delta = r^2 - 2Mr + a^2$):

$$\frac{\partial^2\Psi}{\partial t^2} - \frac{(r^2+a^2)^2}{\Sigma^2}\frac{\partial^2\Psi}{\partial r_*^2} + \frac{4iamMr}{\Sigma^2}\frac{\partial\Psi}{\partial t} + \left[\frac{2a^2\Delta}{r\Sigma^2} - \frac{2iam(r^2+a^2)}{\Sigma^2}\right]\frac{\partial\Psi}{\partial r_*}$$
$$-\frac{\Delta}{\Sigma^2}\left[\frac{\partial^2}{\partial\theta^2} + \cot\theta\frac{\partial}{\partial\theta} - \frac{m^2}{\sin^2\theta} - r\left(\frac{\Delta}{r^2}\right)' - \frac{2iam}{r}\right]\Psi = 0$$

- where

$$\Sigma^2 \equiv (r^2+a^2)^2 - a^2\Delta\sin^2\theta$$

Finite difference methods for 2+1D Kerr

- I've tried various FD schemes for 2+1D Kerr.

	FD method	Variables
Ia	two-step Lax-Wendroff	$\psi, \Pi = \partial_t \psi + b \partial_{r_*} \psi$
Ib	leapfrog	$\psi, \Pi = \partial_t \psi + b \partial_{r_*} \psi$
IIa	iterative Crank-Nicholson	$\psi, \Pi = \partial_t \psi$
IIb	3rd-order Runge-Kutta	$\psi, \Pi = \partial_t \psi$
IIc	4th-order Runge-Kutta	$\psi, \Pi = \partial_t \psi$
III	leapfrog	ψ only

- Problems with numerical instabilities: both radial and angular.
- Method IIc seems most stable (although slow!)

Finite Difference Method for 2+1D Kerr

- Method of Lines: first-order coupled ODEs for Ψ^m, $\Pi^m \equiv \partial_t \Psi^m$.
- Rectangular grid (t, r_*, θ).
- Second-order finite-differencing on spatial slice.
- Fourth-order Runge-Kutta to step forward in time.
- Reasonable stability properties . . .
- . . . but approx. ten times slower than Schw. algorithm!

F_r results for $a = 0.5M$, radii $5M$ to $20M$

r_0	2+1D	freq. dom.	rel err	abs err
5M	-4.162e-5	-4.1602e-5	0.05%	-2.1e-8
6M	-2.426e-5	-2.4217e-5	0.17%	-4.1e-8
7M	-1.471e-5	-1.4677e-5	0.21%	-3.1e-8
8M	-9.240e-6	-9.2191e-6	0.22%	-2.1e-8
10M	-4.038e-6	-4.0352e-6	0.06%	-2.5e-9
14M	-1.073e-6	-1.0757e-6	-0.21%	2.3e-9
20M	-2.543e-7	-2.5026e-7	1.63%	-4.1e-9

Example Kerr Results: Self-Force F_r on the ISCO

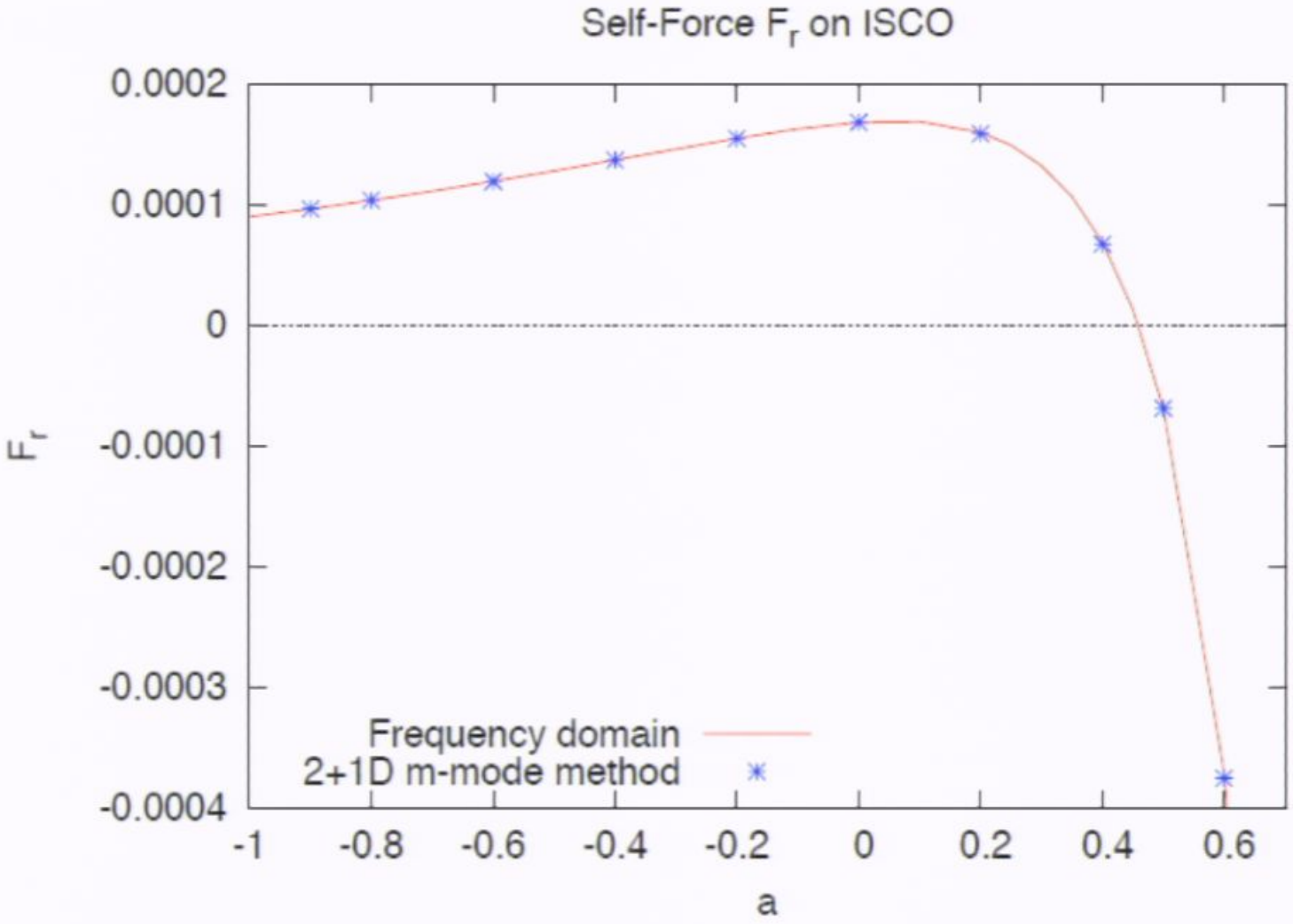

Figure: Comparing 2+1D results (blue dots) against frequency domain results of N. Warburton (red line)

Conclusions

- First demonstration of m-mode regularization method
- First (?) time-domain results for circular orbits on Kerr
- 2+1D approach is competitive alternative to 3+1D approach (c.f. talks by Vega, Wardell, and Deiner).
- Order of puncture $\Leftrightarrow$ mode sum convergence.
- High-order expansion of puncture is key ingredient for accuracy (c.f. Wardell's talk).
- Good accuracy ($\lesssim 0.1\%$) for strong-field circ. orbits ($r \leq 10M$).
- Many interesting future directions ...

Future Directions

- Improvements to Current Implementation
  - 4th order finite difference methods
  - Grid refinement
  - Radial boundary conditions, and/or
  - Horizon-penetrating coordinate systems
  - Faster algorithms? GPUs?
- Scalar SF: Eccentric Orbits in Kerr
  - Highly eccentric equatorial orbits
  - Non-equatorial orbits
- Gravitational SF in Kerr
  1. Lorenz gauge formulation
  2. Circ. orbits in Schwarzschild
  3. Circ. orbits in Kerr
  4. Generic orbits in Kerr